5-5-2012

Development and Application of a Portable System to Reliably Measure Grip Forces Using Thin-Film Force Sensors

Shane Vincent Tornifoglio
University of Connecticut - Storrs, stornifoglio@gmail.com

Development and Application of a Portable System to Reliably Measure Grip Forces Using Thin-Film Force Sensors

Shane Vincent Tornifoglio

B.S., University of Connecticut, Biomedical Engineering, May 2010

A Thesis

Submitted in Partial Fulfillment of the

Requirements for the Degree of

Master of Science

at the

University of Connecticut

May 2012

APPROVAL PAGE

Master of Science Thesis

Development and Application of a Portable System to Reliably Measure Grip Forces Using Thin-Film Force Sensors

Presented By

Shane Vincent Tornifoglio, B.S.

Major Advisor_____

Dr. Donald R. Peterson

Associate Advisor_____

Dr. Anthony J. Brammer

Associate Advisor_____

Dr. Martin G. Cherniack

University of Connecticut

May 2012

Acknowledgements

First I would like to thank Dr. Donald Peterson for welcoming me into the biodynamics laboratory and giving me the opportunity to conduct the research that led to the completion of this thesis. His experience and insight proved invaluable in the experimental design for mapping the hand as well as data analysis. I would like to thank Dr. Anthony Brammer for providing his expertise in the field of vibration and in the portable force unit circuitry design and Dr. Martin Cherniack for providing his insight as to how the grip force may play a role in vibration and the different methods of assessing it. I would also like to thank the National Institute of Occupational Safety and Health for allowing me to use their custom designed grip force handle and funding the research for this project.

I would like to thank all of the members of the Biodynamics Lab for their continued support and encouragement throughout this project. In particular, I would like to thank Takafumi Asaki for introducing me to the force aspect of vibration and machining many parts that were necessary for the completion of this project as well as his continual guidance, Eric Bernstein for his assistance in designing of the force portable force unit and willingness to take the time to help in all aspects of the project whenever needed, and the other members of the biodynamics laboratory Tammy Wojtusik, Jim Gorman, Drew Seils, Tarek Tantawy, Robert Knapp, and Katelyn Burkhart. I'd like to thank Jeff Dussetschleger for his input from a non-engineering background perspective. To the many undergraduate students from the University of Connecticut and University of Hartford who volunteered their time to assist in the project in particular Stephen Elovetsky for his field assistance, thank you.

I would like to thank my family and friends for their continuous encouragement and understanding, in particular my parents, who have offered their continued support no matter the circumstances. Finally I would like to thank Jill Fisk for her never ending faith in me.

TABLE OF CONTENTS

TABLE OF FIGURES

TABLE OF TABLES

Abstract

Accurate tracking of hand grip force is an important consideration needed for a robust understanding in the study of human biomechanics. One aspect where it proves useful is in hand-arm vibration, such as from gripping a power tool. Depending on how firmly the user is gripping the tool, they may change their exposure levels to the tool vibration, which can lead to potential disorders such as Hand-Arm Vibration Syndrome (HAVS).

A small, battery powered portable force unit has been developed to supply power to, and condition, the signals from eight thin-film force sensors. This gives a better understanding of the grip force used on many different tool applications that were previously immeasurable. Using this information, knowledge can be gained in determining how much of a role grip force plays in the onset of the aforementioned disease.

Using the portable force unit, two different applications are explored. The first uses an instrumented handle in conjunction with thin-film sensors to ascertain how well the thin-film sensors model the overall grip strength recorded by the handle. Using varying numbers of sensors to map the hand, a conversion factor was determined to calculate the actual grip force represented by the waveforms of the thin-film sensors. The observed results of this experiment indicated that the use of eight to four thin-film force sensors yield conversion factors that are similar, therefore using four sensors gives a similar estimated force response, while minimizing sensor bulk.

The second application is in field work. Several grip force measurements were made in the field while subjects were using pneumatic power tools. A subject calibration

of the thin-film sensors was performed using the same instrumented handle mentioned previously and the unit allowed for the thin-film sensors to be used in the actual tool use measurement. Using the conversion factors from the laboratory on the data collected in the field, a better understanding of grip force was obtained. This understanding is from a real work environment rather than a laboratory tool simulation conducted by lab personnel unfamiliar with the tool, which could bias the results. Applying this method of tracking grip force is expected to provide a better understanding of how grip force plays a role in HAVS and how tool handle designs can be improved.

1. Introduction

Accurate and robust tracking of hand grip force is an important consideration in the study of human biomechanics. One aspect where it proves useful is in hand-arm vibration, such as from gripping a power tool. Depending on how firmly the user is gripping the tool they may change their exposure to the tool vibration, which can lead to potential disorders such as the Hand-Arm Vibration Syndrome (HAVS). Several studies have been completed, which use various methods to determine how grip force relates to vibration.

1.1 Force Sensor Measuring

One of the first methods developed to measure real-time, day long force on the hand involved the use of a small, portable data-logging system, designed by Peterson et al. (2008), that measured acceleration and force from a palm-mounted adapter, which contained an accelerometer and a force sensor. The system measured tool-operating times, hand-transmitted vibration, and palm forces throughout a representative sample of an eight-hour work day. The data-logging allowed for simplicity and robustness in the field and eliminated the need for hand simulations in a laboratory. Although this system was originally intended to measure vibration, it was one of the first systems capable of measuring hand forces in a work environment, real-time, throughout all, or a representative part, of an eight hour work day.

Lemerle et al. (2008) took another approach to measuring grip forces that involves a pressure mapping technique that would also indicate push forces. The study investigated how much precision could be expected from the pressure mapping technique for the determination of coupling forces by means of numerical integration. A procedure

was developed and validated to instrument hand-held tools and measure coupling forces. The method was applied to a case study of a breaker (i.e. jack hammer) and anti-vibration breaker. This pressure mapping showed promise in the future provided that the operator accounted for bending of the sensor and that enough pressure was applied to register a reading on the sensor.

Mentzel et al. (2011) used a sensor glove to assess force patterns of different primary grips through dynamic force measurements. Ten subjects were examined using a TUB-sensor glove (FSR 151, Conrad Electronics, Hirschau, Bavaria), which was equipped with ten pressure sensors: five at the metacarpophalangeal (MCP) joints and five at the distal interphalangeal (DIP) joints. Nine different grip motions were examined and could be classified into two categories: power and precision. For the power grips, the force distribution was shifted further distally with increasing size in the object being grasped. It was found that as the size of the object being grasped increases, there was a shift towards the precision grip, where the thumb plays more of a role.

1.2 Force Sensor Approach

There have been a number of studies that use instrumented grip force handles as their method of measuring. The grip handles typically act as a reference because, in most cases, these handles cannot be used at the same time as the action being investigated, such as in power tool operation. In this case the handle provides surrogate measurements of force; however, for studies where the handle was used in laboratory settings and there was no action being referenced, the handle served as an ideal grip force measurement device as it captured the entire contact area of the hand and thus the entirety of the grip force measurement.

Chadwick et al. (2001) introduced a new strain gauge transducer that had been developed to measure functional grip force. The gripping area was a cylinder with a diameter 30 mm and length of 150 mm simulating the handle of a number of other devices and allowed for a range of activities to be studied. The gripping handle developed measures radial forces divided into six components and is capable of measuring forces up to 250 N per component. This handle is unique in that it not only gives magnitude, it also gives the distribution information about the force around the cylinder during gripping. The handle design was the basis for the handle eventually used in this study.

Wimer et al. (2009), part of the National Institute of Occupational Safety and Health (NIOSH), developed a dynamometer for measuring grip strength similar to that of Chadwick et al. The intent was to enhance the understanding of hand grip force applied to a cylindrical handle and develop a new dynamometer for measuring maximum grip force. The NIOSH-owned, instrumented cylindrical handle developed measures 40 mm in diameter and has six measuring beams. Preliminary studies showed that, while friction forces do exist in the gripping action, their levels are not comparable with the normal forces, and can be ignored. No reliable correlation between the developed handle and the clinically-used Jamar (Jamar, Lafayette Instruments, Lafayette, Indiana, USA) handle dynamometer was observed. This suggests that the grip strength measured with the Jamar handle may not always be applicable to the design and risk assessment of some tools or machines with cylindrical handles. The handle showed overall grip force as well as grip force distribution around the circumference of the handle. It was also shown that

the handle was accurate to within four percent, independent of the loading position along the handle.

1.3 Thin-Film Sensor Applications

While the handle technique is well suited for reference measurements, it cannot be used in the field on the subjects doing the activity being studied. There is a need to develop a small, portable sensor that can be used while working to record actual field measurements. The studies discussed below examine the use of thin-film sensors and their application to force monitoring applications.

Ferguson-Pell et al. (2000) evaluated a new force sensor to the market, the FlexiForce (FF) (A101, Tekscan, Boston, MA), for low interface pressure applications. The study focused on drift, repeatability, linearity, hysteresis, and curvature effects of the FF sensor in laboratory conditions. It was found that the drift was 1.7-2.5% per logarithmic time, repeatability was 2.3-6.6%, and the linearity was 1.9-9.9% for the 10 to 50 g loads applied. The hysteresis was found to be 5.4% on average. The output offset of the sensor increased with decreasing radius of curvature for radii less than 32 mm compared to a flat surface when no pressure was applied. Sensitivity decreased with curvature for radii less than 32 mm. As a result, the sensor was deemed acceptable for static measurements on surfaces where the radius was greater than 32 mm, but not where the surface has a radius of curvature equal or less than 32 mm.

Lebosse et al. (2008) studied several thin-film peizoresistive sensors such as Tekscan's FlexiForce and Interlinks Force Sensing Resistor (FSR) (402 FSR, Interlink Electronics, California, USA). The focus was on low cost sensors that were considered to be an alternative to the typical commercial force sensors such as load cells, which are

bulky and more expensive. An experimental study of the static and dynamic behaviors of the sensors was conducted. There was a particularly strong interest in the nonlinearities of their dynamic behavior. The nonlinearities were identified and a compensation model was developed. Through testing of the compensation model it was found these sensors can be used in the presence of a strong magnetic field and, therefore are of great interest for medical applications.

Khaburi et al. (2011) performed one such medical application. The study investigated the pressure being applied by nurses when dressing patients with medical compression bandages. The FF was compared with the traditional PicoPress (MicroLab, Roncaglia of Ponte San Nicolò, Italy) pneumatic transducer as well as a FS01 (FS01, Honeywell, New Jersey, USA), which is an ultra-profile rigid MEMS force sensor. The FF was organized into an array to cover more area than the single point of just one force sensor. With the array configuration, the FF provided more detail about distribution than the other two sensor types being studied. In addition, it also proved to be more cost effective.

Ouckama et al. (2011) demonstrated another use of FF sensors in medical applications. They investigated the interaction between the head and athletic helmets with regards to contact area and force. The study evaluated a system to capture the impact force distribution of helmet foams. The FF sensors were used in a 5x5 cm array, which covered 36% of the total foam area, and was secured to a load cell. Using an array provided greater insight into the distribution patterns of contact area and forces on impact between the head and the foam. This type of information is valuable in designing helmet

foam that will decrease the number of head injuries which result from head to helmet contact.

Thin-film sensors can also be used to examine hand forces, including grip force using tools. Lu et al. (2008) investigated the hand forces and postures for using mechanical pipettes. In particular the study evaluated thumb and hand forces as well as posture at the wrist, forearm, and shoulder for the use of three different mechanical pipettes. Twelve subjects participated in the pipette simulations and the thumb and hand forces were measured using 19 FF sensors. It was found that a non-axial pipette was associated with approximately two to six times less thumb and hand force than the traditional axial pipettes. These results may provide information for hand injury prevention as well as tool design for pipettes in the future.

Nikonovas et al. (2004) claimed to be one of the first studies that not only placed the sensors on the hand rather than the object, but also mapped the entire hand rather than just the finger tips. The ultra-thin FF sensors were used in the study as well. Sixty sensors, sampled at a rate of 400 Hz per sensor, were used to examine several everyday activities such as driving a vehicle, lifting saucepans, and hitting a golf ball with a golf club. They suggest that their results of mapping the entire hand gives useful information about future tool design and applying the sensors to the hand rather than the tool gives better force distribution results.

1.4 Handle & FlexiForce Combination

After examining several methods that measure grip force with instrumented handles and with thin-film sensors, attempts to combine both methods were extremely limited. Marcotte et al. (2011) proposed a low cost system that evaluated coupling forces

on real power tool handles using both systems. It was hypothesized that the grip and push forces can be estimated using two single distributed force sensor elements: one positioned between the palm and the handle and the other between the fingers and the handle. Tekscan designed a custom FF sensor for this system and a test was performed on a split handle 40 mm in diameter. The handle was then mounted on a shaker to measure grip and push forces. The results of the study suggest that the sensor is capable of estimating the grip and push force on a cylindrical handle. This study combined the instrumented handle technique with the point force measurements and allowed for the simultaneous measuring of the grip force using the different methods.

1.5 Gloves Influence on Grip Force

An individual's grip strength can be influenced by several factors including the use of gloves and hand size. There are many different types of gloves that are used in industry and some jobs require gloves that are padded for protection from either vibration or sharp edges, while others require thinner gloves with more emphasis on grip to allow for better handling of materials. Several studies have investigated the effects of gloves during activities involving grip. For example, Slane et al. (2011) investigated the influence of glove and hand position on pressure over the ulnar nerve during cycling. The study quantitatively evaluated the effects that hand position and glove type can have on the nerves in the hypothenar regions of the hand. Thirty-six experienced cyclists participated in the study with their hands placed in three different positions: the tops, the drops, and the hoods of a standard drop handlebar. A high resolution pressure mapping system was used to record hand pressure with no gloves, unpadded gloves, foam-padded gloves, and gel-padded gloves. Laser scans of each subject's hand were acquired to

register the pressure mapping to the hand anatomy. The results show that the padded gloves were able to reduce hypothenar pressure magnitudes by 10 to 28%, with the foam-padded gloves showing slightly better results than gel-padded. As a result, the study recommended that cyclists should use padded gloves to reduce the amount of pressure on the ulnar nerve in the hypothenar region of the hand.

Seo et al. (2010) studied the effects of handle orientation, gloves, and posture on maximum horizontal push and pull forces. Several biomechanical models were evaluated for the effects mentioned. Eight subjects performed maximum push-pull exertions on handles of different materials and orientation, while varying two different postures and using two different types of gloves or no gloves. It was found that cotton gloves reduced the forces by a significant amount, while the polyvinyl chloride (PVC) glove influenced the forces to a lesser extent. It was thought that the cotton gloves were thicker and had more cushion, which changed the distribution of the forces and, thus, the overall resultant force.

Wimer et al. (2010) wanted to establish an alternative method for measuring the effects of gloves on the grip strength applied to cylindrical handles and to quantify the strength reduction due to the use of typical anti-vibration (AV) gloves. The alternative method was to measure the total contact force normal to a cylindrical handle. Two handles were used with diameters of 30 and 40 mm. Ten subjects participated in the study to analyze four different types of AV gloves in comparison with two types of non-AV gloves. The results showed that the AV gloves reduce the total grip strength by more than 29% regardless of the handle size. One of the non-AV gloves had a similar effect, reducing the grip strength by 25%. The last non-AV glove reduced the total grip strength

by less than 10%. It was also seen that the gloves influenced the force distribution pattern around the circumference of the cylindrical handles. The results suggest that the thickness of the glove is a major factor associated with these effects. The thicker the glove the more the total grip strength is reduced, which makes the forces more evenly distributed.

1.6 Hand Size Influence

Another factor that may determine grip force is the hand size of the subject and several studies have investigated how much of a role, hand size actually plays. Ruiz-Ruiz et al. (2002) investigated different grip positions on the standard dynamometer. Using maximum grip strength data, which was recorded from the dynamometer, they intended to derive a simple mathematical algorithm to account for grip span and hand size. Seventy subjects (40 women and 30 men) participated in the study that incorporated five different grip spans. Each hand for each subject was evaluated ten times and the findings demonstrated that one optimal grip span was identifiable for both genders and hand size. It was also found that optimal grip span correlated with grip force in women but not men and that hand size must be taken into account, especially when measuring hand strength in women.

Seo et al. (2008) investigated the relationships between grip force, normal force, contact area, handle size, and handle diameter for cylindrical handles. The study was a review of the data from other studies using handles measuring 38 to 83 mm, while grip force, normal force, and contact area were recorded. The length, width, and volar hand area were also measured. It was found that the total normal force on cylindrical handle was 2.3 times greater than grip on a split cylinder handle, regardless of diameter. This

reinforces the belief that traditional one-dimensional grip force measurements are insufficient for use in tool design. The ratio of handle diameter to hand length explained 62%, 57%, and 71% of the variances in the grip force, normal force, and contact area, respectively. The estimated hand area (i.e. the product of the hand length, L, and the hand width, W) had a linear relationship with the measured hand area even it was 8% less than the measured area. This study shows that there may be some relationship between hand length and handle diameter when compared to the forces measured. This information may be clarified further to better understand how to make tools or gloves fit a higher percentage of the population's hands to protect the users from injury and disease.

1.7 Grip Force Models

Using some of the methods previously mentioned, there have been several studies that focus on grip forces determined in field settings or in a laboratory setting where field work with power tools is simulated. Burström et al. (1997) investigated the influence of several biomechanical factors on the mechanical impedance of the hand-arm system. The hand-arm system was studied during exposure to random vibration under various experimental conditions to statistically evaluate whether the experimental conditions have any influence on mechanical impedance. Ten subjects were studied under varied conditions including vibration direction, grip force, feed force, frequency-weighted acceleration, and hand-arm position. It was found that increased grip force and feed force lead to increased impedance for all frequencies. This is understood as reducing the signal magnitude, but not necessarily the exposure levels. This raises the question of whether grip force changes the exposure to vibration.

Lin et al. (2003) took a more direct approach, studying one specific tool. Pneumatic power screwdriver operations were studied with a focus on predicting the forces acting on the human. A static model was proposed based on the tool mass, geometry, orientation, feed force, torque build up, and stall torque and three handle shapes were considered for the model: pistol, right angle, and inline. A dynamic model was also developed to describe the pneumatic motor torque build-up characteristics, which were observed to be dependent on the hardness of the threaded fastener joint. Six pneumatic tools were then tested to validate the deterministic models, which predicted forces to within 7%. These models may be helpful in considering tool handle force in selection and design of power screwdrivers.

Other studies investigate the change in worker effort during activity involving grip force. Buchholz et al. (2008) examined the agreement of subjective ratings of upper extremity exposures with corresponding direct measurement obtained simultaneously from workers. The study used the Borg CR-10 scale for psychophysical exposures and shoulder and wrist posture data were also collected with the grip force data as the primary focus of the study. The Borg scale is a method of physical intensity force approximation using a qualitative assessment. The ratings of manual effort were significantly correlated with directly measured grip force. The ratings of pace (i.e. being rate of work), were strengthened with the addition of relative grip force as a statistical covariate. This shows that grip force is a strong indicator of the amount of effort exerted during a given activity.

Li et al. (2011) also used the Borg CR-10 scale when examining the relationship between grip force and four levels of the scale under experimental conditions. It was determined that subjects applied a higher grip force than perceived at levels 2, 5, and 7.

The grip force differences between dominant and non-dominant hands at low CR-10 levels were negligible; however, at level ten, the differences were significant. Estimated ratings were lower than those actual values under all of the tested conditions. This is may be to fatigue, since at a rating of ten, the maximum grip force is exerted and may be difficult to consistently reproduce. A different study by Dale et al. (2011) addresses the misclassification of workers estimation of force by overestimating. The investigation uses dynamometer force measurements to estimate worker hand force. The validity of worker estimates of hand force in a field study was evaluated to determine the misclassification of worker estimates of hand force exposures compared to directly measured forces. Eight sheet metal assemblers completed quarter inch fastener installations using six different pneumatic tools. A pressure mat was used to record grip forces, which were then compared to worker estimates using on a dynamometer. The results indicated a fair to moderate correlation, with the estimations being higher than the measured results. This demonstrates that there may be some factors, such as experimental validity, that can influence simulation measurements that are not made directly on the tool during actual work. This suggests a need to better evaluate the relationship between actual grip measurements and estimated grip measurements as these two investigations arrived at opposite conclusions.

Grip force measurements can also be applied to non-work activities, such as driving a car. Eksioglu et al. (2008) investigated grip force on 13 subjects as a function of gender, speed (45 and 65 mph), and two road conditions (smooth and rough asphalt). The grip force measurements used a custom-made capacitive pressure mapping system wrapped around each steering wheel. The results of the study indicated that male drivers

had a significantly higher grip force than females. Driving speed and road conditions did not influence the response variables and it was found that on average the subjects applied 31% of their total grip strength when driving. This demonstrates that measurable grip forces are present in everyday tasks, such as driving.

The majority of studies dealing with grip force are related to power tools. Lin et al. (2010) investigated power tools with the potential to produce reaction forces that may be associated with upper extremity musculoskeletal disorders. Comparisons between kinetic and physiological impacts on the operator's upper extremities between fastening and unfastening operations were examined in 32 right-handed male operators using four tools on two joint simulators at different working heights and distances in the laboratory setting. Grip force was measured on an instrumented handle attached to each tool and muscle activity in the forearm was also monitored. The results indicated that the average grip force corresponded with peak tool torque and suggested that the effort to react against tool torque was greater in the unfastening cycles rather than the fastening cycle for all work configurations. This study shows that the more torque the tool exhibits, the tighter the grip must be. The study concluded that the fastening and unfastening activities have the potential to increase risk for musculoskeletal disorders.

1.8 Anatomy of the Hand

An understanding of how the hand functions to grasp objects is necessary to fully comprehend the injuries and diseases that can be associated with gripping. The gripping action occurs in digits two through five and, in order to keep the object grasped, the forces need to be opposed equally by either the palmar aspect of the hand or the first digit, depending on the size of the object and the grip being used. The larger the object,

the more of a role the first digit plays in the gripping action. Figure 1 is an overview of the bones in the human hand showing the digits, palm, wrist, and carpal arch as well as the joints of the hand and wrist.

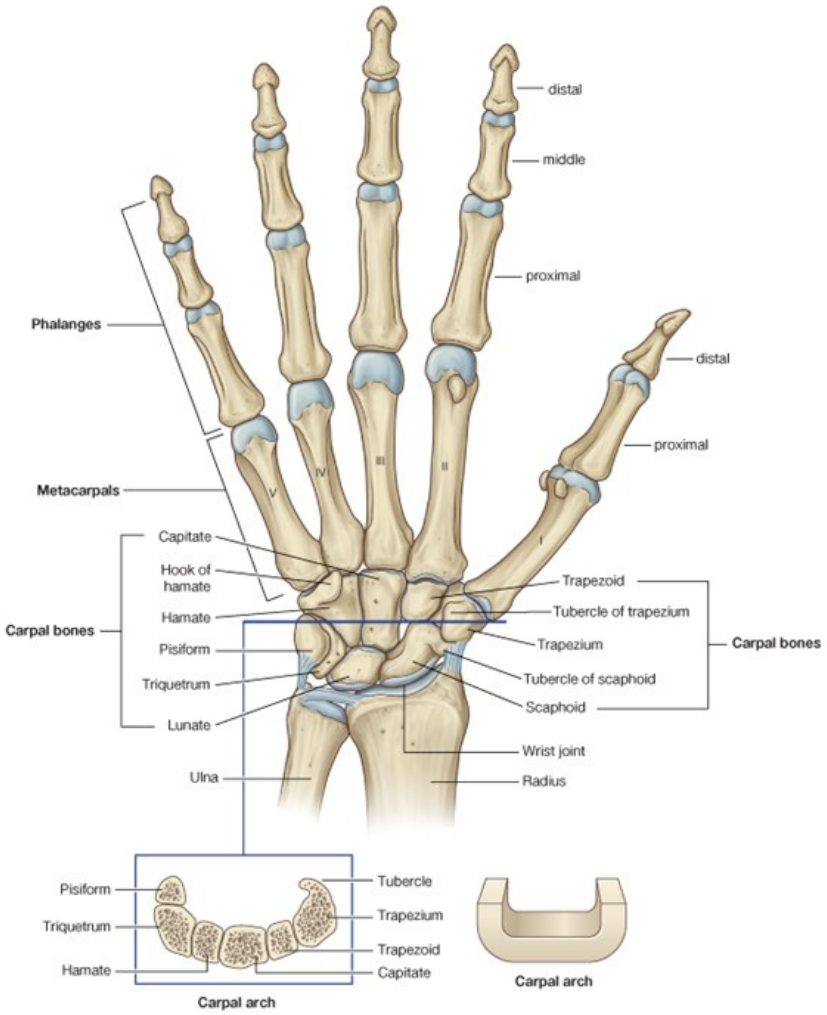

Figure 1: Bones of the hand and wrist joint. (Gray, 2010)

The wrist is a synovial joint between the distal end of the radius, distal end of the ulna, and the scaphoid and lunate, which have limited movement. The wrist joint allows movement around two axes; abduction and adduction, and flexion and extension. The carpal joints are the synovial joints between the carpal bones and they are reinforced by numerous ligaments. There are five carpometacarpal joints between the metacarpals and

the related distal row of carpal bones. The MCP joints are the joints between the distal heads of the metacarpals and the proximal phalanges of the digits. These are condylar joints which allow flexion, extension, adduction, abduction, circumduction, and limited rotation and are reinforced by the palmar and collateral ligaments. Finally there are the interphalangeal joints of the hand that are hinge joints that allow for flexion and extension, which are also reinforced by palmar and collateral ligaments.

The muscles in the forearm are what provide power to the digits and palmar aspect of the hand to grasp tools, while the muscles in the hand do not generate grasping power. The more muscle contraction and recruitment, the stronger the grip will be. The muscles receive their oxygen and energy from the blood supply, which is carried by the blood vessels. There are two main arteries that provide the oxygen rich blood supply to the hand and its muscles. The first is the ulnar artery, which supplies blood to digits three, four, five, and their respective tissues, and the second artery is the radial artery, which is responsible for supplying blood to the first and second digits and their respective tissues. Veins are vessels that return the oxygen poor blood back to the heart and lungs to be resupplied with oxygen and have return paths similar to that of the arteries supply. The artery supply route can be seen in Figure 2 and the venous network can be seen in Figure 3.

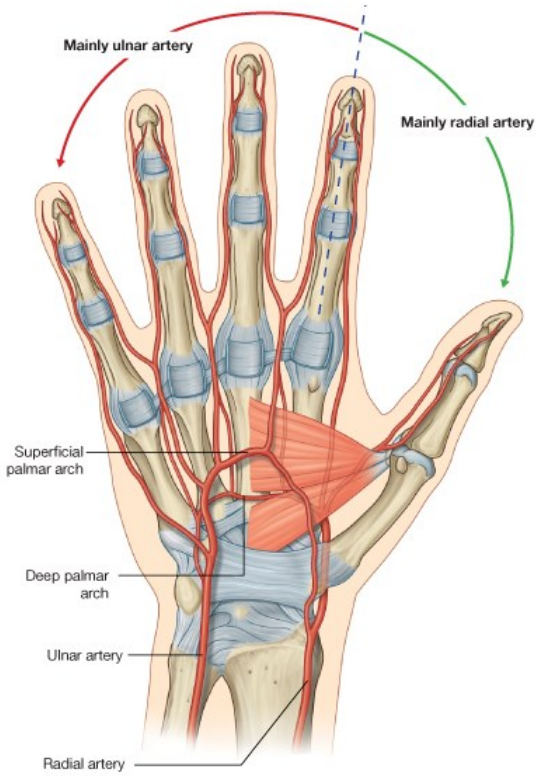

Figure 2: Arterial blood supply to the left hand. (Gray, 2010)

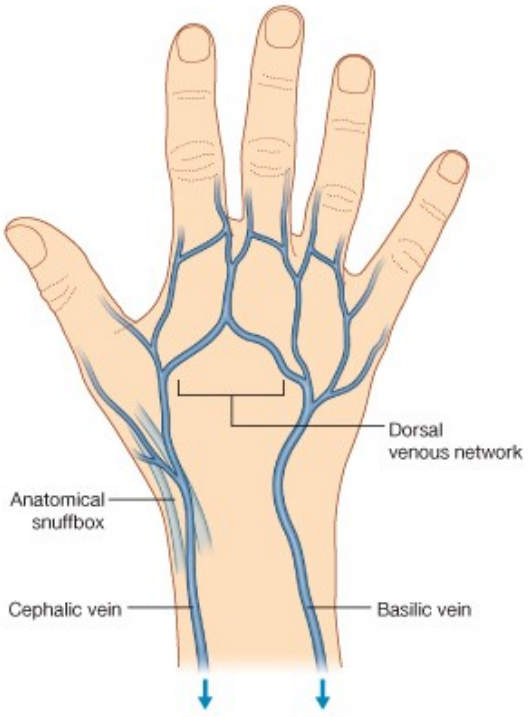

Figure 3: Dorsal view of the venous network of the right hand. (Gray, 2010)

There are three nerves that innervate the hand. The ulnar nerve travels parallel to the ulnar artery and provides motor and superficial sensation for the fifth digit, part of the fourth digit, and the hypothenar region. The median nerve is thought of as the most important sensory nerve in the hand because it innervates skin on the first, second, and third digits. The nervous system gathers information about the environment from this area, primarily from touch. In addition, sensory information from the lateral three digits enables fingers to be positioned with the appropriate amount of force when using precision grip. Only the superficial branch of the radial nerve enters the hand and it innervates skin over the dorsolateral aspect of the palm and the dorsal aspect of the first three digits. The nerves of the hand can be seen in Figures 4, 5, and 6 along with their respective sensory areas.

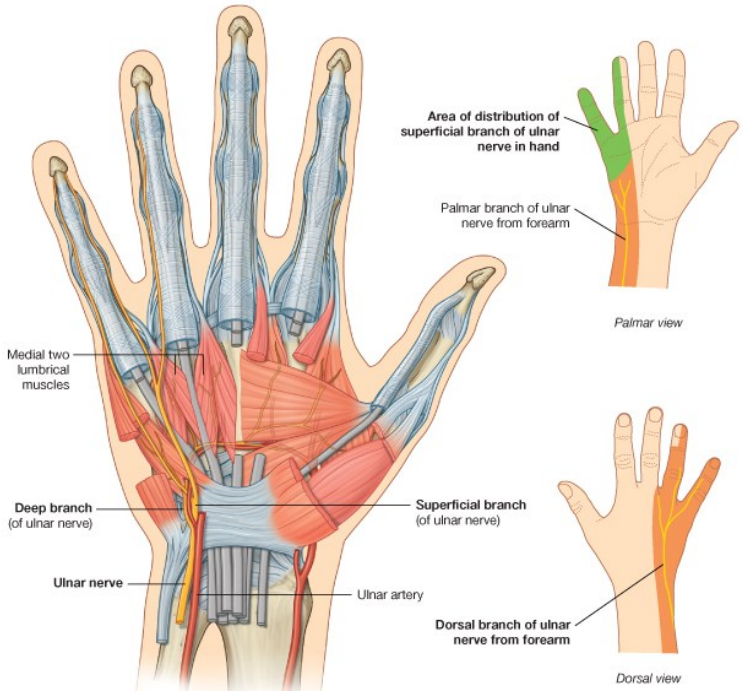

Figure 4: Ulnar nerve of the left hand. (Gray, 2010)

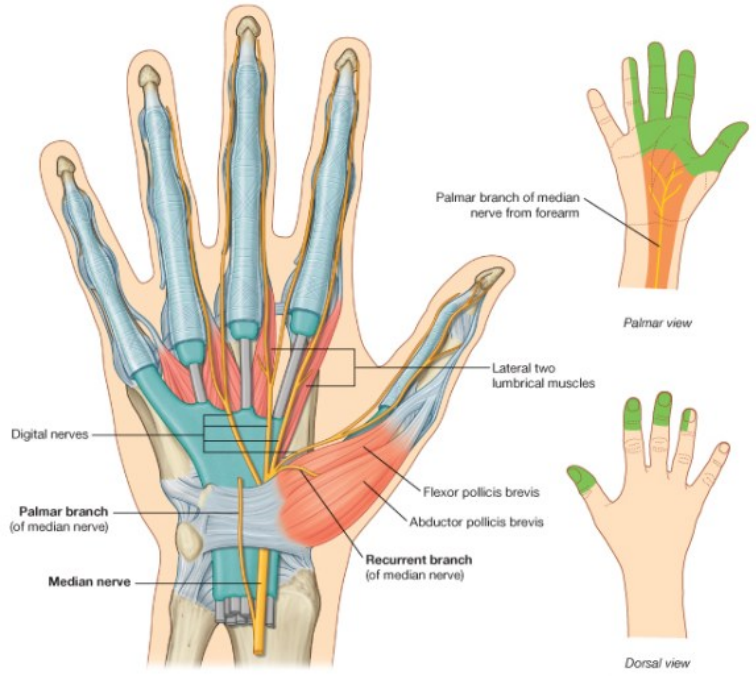

Figure 5: Median nerve of the right hand. (Gray, 2010)

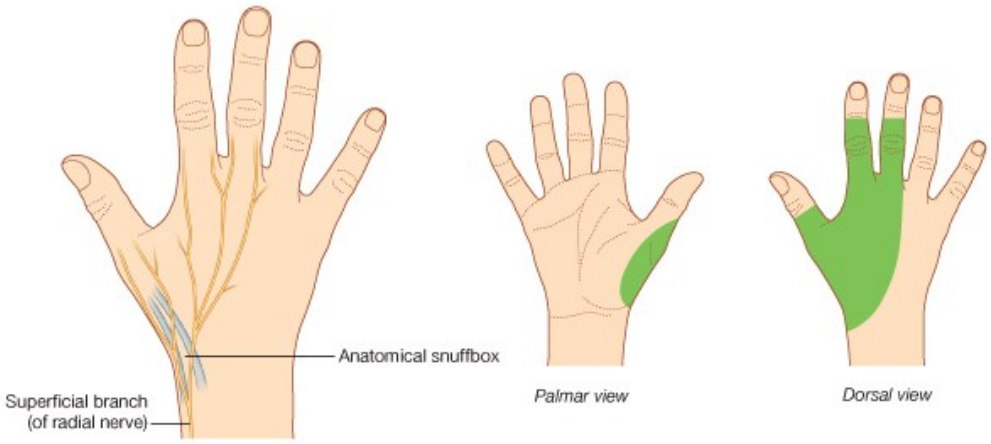

Figure 6: Superficial branch of the radial nerve in the right hand. (Gray, 2010)

1.9 Injury and Disease

There are many different types of injuries and disease in the hand that can influence grip force. Most of these diseases are either nerve or muscle degenerative diseases such as Huntington's disease or Lou Gehrig's disease (Amyotrophic lateral sclerosis (ALS)). The number of diseases that are caused by physical labor are more

sparse and generally depend on the type of work being conducted. Two diseases are of particular interest when it comes to the hand and grip force: carpal tunnel syndrome and Hand-Arm Vibration Syndrome (HAVS), which is synonymous with vibration-white finger.

The carpal tunnel is located at the anterior of the wrist by an arch formed of the carpal bones and the flexor retinaculum. Carpal tunnel syndrome is an entrapment syndrome caused by pressure on the median nerve within the carpal tunnel with diverse etiology. In some instances the nerve injury may be a direct effect of increased pressure on the median nerve caused by overuse, swelling of the tendons and tendon sheaths (rheumatoid arthritis), and cysts in the carpal joints. It is thought that the increased pressure in the carpal tunnel causes venous congestion, which can produce nerve edema and damage to the median nerve itself. Patients typically report pain, described as a 'pins-and-needles' feeling in the median nerve and the loss of muscle volume causes reduced grip strength. The best treatment is preventive, such as changing certain habits, actions, or potentially even jobs that may reduce inflammation and pain. If these actions are not enough, a surgical option may be necessary to reduce pressure on the nerves.

HAVS is a disease that is associated with vibration exposure. There are many different factors associated with the development of the disease, such as temperature, which is an environmental factor. If the working environment is cold, there is a greater likelihood of developing HAVS than if the environment is warm. Other factors include the vibration frequency as well as the vibration magnitude, which is dependent on the tool or equipment being used. Equally important is exposure or how much time the user spends with each vibrating tool. The risk increases if the hand-arm system is exposed to

too much vibration energy within a certain time frame. The symptoms of HAVS include numbness, tingling, and loss of nerve sensitivity and in severe cases the disorder is very painful and can potentially lead to loss of finger, hand, and arm function. The disease begins with a tingling sensation and numbness in the fingers, which then become white and swollen when cold and then red and painful when warmed again. Picking up small objects such as nails or pins becomes difficult as the feeling in the fingers diminishes and there is a loss of strength and grip in the hands. Depending upon the severity of the symptoms it can eventually interfere with sleep. HAVS can be caused by a number of different vibration sources, such as a drill to a jackhammer to an electronic game where vibration is transmitted to the tissue of the hand. The disease causes the nerves and the blood vessels to degenerate, causing a lack of blood flow and painful sensations, which then causes the muscles to degenerate and weaken. The loss of force generation is a result of the combination of weakened muscles lacking strength and damaged nerves sensitivity feedback. The affected hand can even turn white where the damaged nerves and vessels are innervated. The pain originates from the damaged nerves and the whiteness is a result of the loss of blood flow. Whether or not the amount of force used to grip the tool plays a role in the onset of the disease is still unknown.

1.10 Thesis Objectives

To explore the effects of hand grip force on vibration exposure, a small, battery powered, portable force unit has been developed to allow field measurement from eight thin-film sensors mounted on the hand. This unit can provide a better understanding of the grip force used on many different tool applications that were previously

immeasurable. Using this information, it is hoped to gain a better understanding of the role that grip force plays in the onset of diseases such as HAVS.

Using the portable force unit, two different applications are explored. The first uses an instrumented handle in conjunction with thin-film sensors to ascertain how well the thin-film sensors model the overall grip strength recorded by the handle. Using varying numbers of sensors to map the hand, a conversion factor can be determined to calculate the actual grip force represented by the component waveforms of the individual thin-film sensors.

The second application is in field work. Several grip force measurements were made in the field while subjects were using pneumatic power tools. A subject calibration of the thin-film sensors was performed using the same instrumented handle mentioned previously (Wimer, 2009). The unit allowed for the thin-film sensors to be used in the calibration as well as the actual tool use measurement. Using the conversion factors from the laboratory study on the data collected in the field, a better understanding of grip force can be obtained. This understanding is from a real work environment rather than a laboratory tool simulation conducted by lab personnel unfamiliar with the tool, which could bias the results. Applying this method of tracking grip force is expected to provide a better understanding of how grip force plays a role in HAVS and how tool handle designs can be improved.

2. Methods

The FlexiForce (FF) (A101, Tekscan, Boston, MA) sensor was selected as the thin-film sensor best suited for monitoring hand grip force due to its small size, linear response, and repeatability. The portable force unit provides the power, filtering, and amplification necessary for field operation of eight FF sensors but requires an external analog-to-digital converter (ADC) for capturing force waveforms.

2.1 Portable Force Unit Design

The desired output specification of the signal conditioning unit was required to have an output voltage between 0 to 5 V that linearly corresponds with force ratings from 0 to 100 lbs. The FF sensor linearly relates the force applied to the sensor element in terms of output electrical conductance. To accomplish the linear relationship between conductance and voltage, an inverting operational amplifier circuit was implemented and the configuration recommended by Tekscan is illustrated in Figure 7. The equation for an inverting operational amplifier is

$$V_{out} = -V_{in}\left(\frac{R_{ref}}{R_{sens}}\right), \qquad (1)$$

where $V_{out}$is the voltage output, V_{in} is the source voltage, R_{ref} is the reference resistor for gain control, and R_{sens} is the resistance of the FF sensor. Since conductance is the inverse of resistance and the sensor linearly relates force to conductance rather than resistance, this equation simplifies to

$$V_{out} = -V_{in}\left(R_{ref} * G_{sens}\right), \qquad (2)$$

where G_{sens} is the conductance of the FF sensor. It is important to note that the output voltage has the opposite sign of the input voltage; therefore, in order to have a positive output voltage, the supply voltage,V_{in} must be negative. In typical inverting operational

amplifier applications, V_{in} is the input variable and V_{out} is the output variable; however, in this application where the sensor's output is in terms of conductance, G_{sens} is the input variable, while V_{out} is the output variable and V_{in} and R_{ref} are constants.

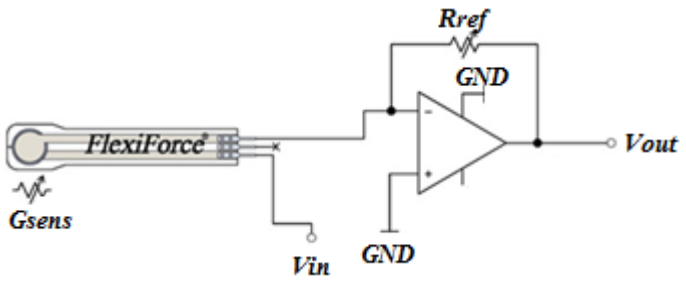

Figure 7: FlexiForce sample circuit (http://www.tekscan.com/flexible-force-sensors)

The circuit of the signal conditioning unit starts with a voltage supply from eight AA batteries, which is fed into a 5 V regulator to provide a constant 5 V source for the operational amplifiers and the DC/DC converter. The converter changes the 5 V supply to the -5 V used to power the sensors. The signal conditioning circuit is repeated eight times for each of the eight sensor channels. The first of three stages of signal conditioning starts with the inverting amplifier circuit in Figure 7.The gain resistor was made in a socket so that the gain can be controlled and changed easily. The second stage of the circuit, illustrated in Figure 8, is a second order low pass filter with a cutoff of 20 Hz and a gain of exactly two (Mancini, 2009).

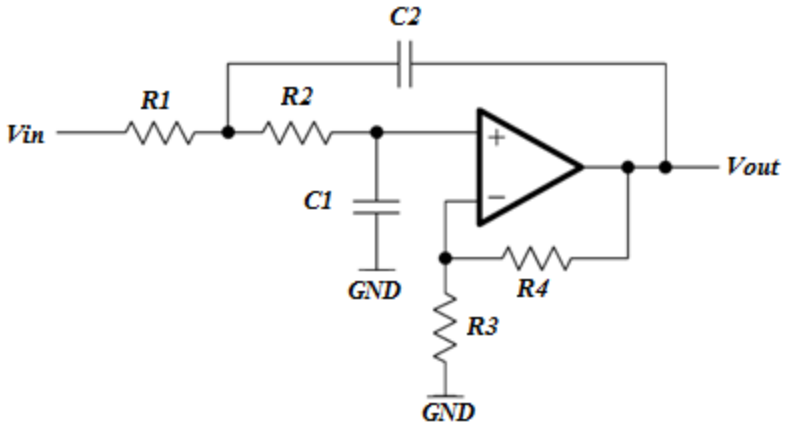

Figure 8: Second-order low pass filter. (Mancini, 2009)

The following equation is the transfer function for the second-order low-pass filter in the Laplace domain

$$A(s) = \frac{A_0}{1+(C_1(R_1+R_2)+(1-A_0)R_1*C_2)*s+R_1*R_2*C_1*C_2*s^2}, \quad (3)$$

where s represents jω, $A(s)$is the transfer function, and the gain $A_0$is (1+R_4/R_3). Ordinary frequency can be related to angular frequency with the following

$$\omega = 2 * \pi * f, \quad (4)$$

where f is the ordinary frequency in Hertz and ω is the angular frequency in radians per second. The cutoff frequency is specified and then solved for using Equations 5 and 6 to give specific component values.

$$R_{1,2} = \frac{a_1*C_2 \mp \sqrt{a_1^2*C_2^2-4*b_1*C_1*C_2}}{4*\pi*f_c*C_1*C_2}, \quad (5)$$

$$C_2 \geq C_1 * \frac{4*b_1}{a_1^2}, \quad (6)$$

where $a_1 = C_1(R_1 + R_2)$ and $b_1 = R_1 * R_2 * C_1 * C_2$. Finally, the signal is passed through a voltage buffer circuit to provide a low impedance output into an external A/D converter. Figure 9 is a block diagram of the total circuit.

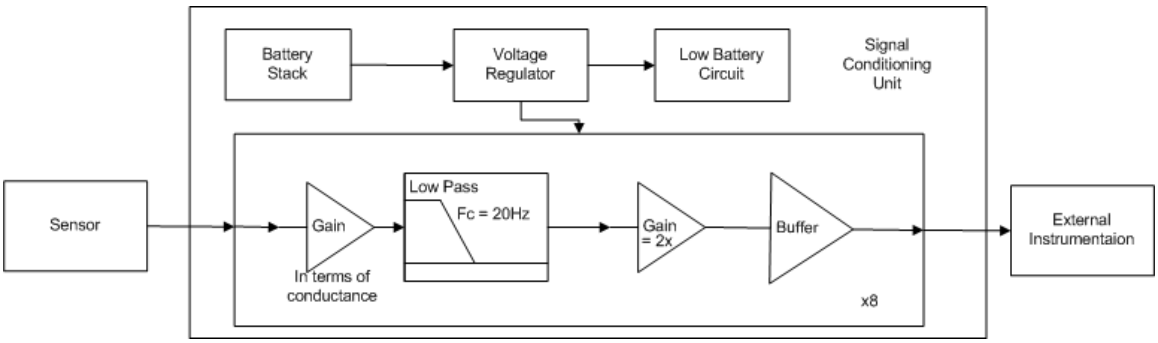

Figure 9: Block diagram of the portable force unit system

A low-battery circuit was added to indicate when the battery levels approached voltages that would prevent the unit from working properly. The low voltage limit was determined by the regulator drop out voltage, 6.5 V. When the power button is pressed and the indicator light remains solid, this indicates that battery power is sufficient. If the power button is pressed with no indicator light, then the batteries need to be charged or replaced.

2.1.1 FlexiForce Sensors

The FF sensors chosen for this study are flexible, ultra-thin-film printed circuits. The sensors come in varying lengths from 51 mm to 197 mm, and are 14 mm wide and 0.203 mm thick with a sensing area that is a circle measuring 9.53 mm in diameter. The change in resistance of the sensing element is inversely proportional to the applied force and since the conductance is the inverse to resistance, the conductance is linearly proportional to this applied force.

The sensing area functions through pressure sensitive ink on both sides of the sensor connected to a conductive silver strip. The greater the force applied to the sensing area, the more the ink comes into contact with the ink on the opposite side of the sensor, where increasing ink contact leads to less resistance between the two sensing areas and increased current flow.

In order to maximize pressure on the sensing area, the sensors were modified with custom made 'pucks' that were constructed to match the size of the sensing area and better distribute force over the area. These pucks were adhered to the sensing area and then medical tape was used to cover the sensor and the puck to localize the forces applied to the sensing area and to make the sensor more durable. An original sensor and a modified sensor can be seen in Figure 10.

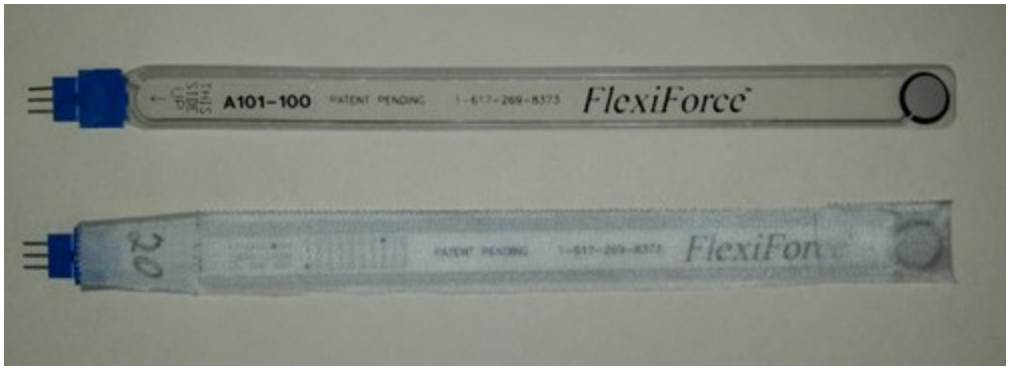

Figure 10: Top - A new FF sensor prior to the custom modifications made. Bottom - The FF sensor after the modifications have been made

Calibration - There were a number of methods that had been proposed and implemented for calibration. The first of these methods involved a system that had a plate suspended over two saw horses. The top of the plate had a custom designed fixture that localized all of the force from the plate onto the sensing area of the FF sensor. String was used to attach the plate to the fixture and weights were then placed on the plate. This calibration method was somewhat unstable and difficult but was observed to be effective at calibrating and can be seen in Figure 11.

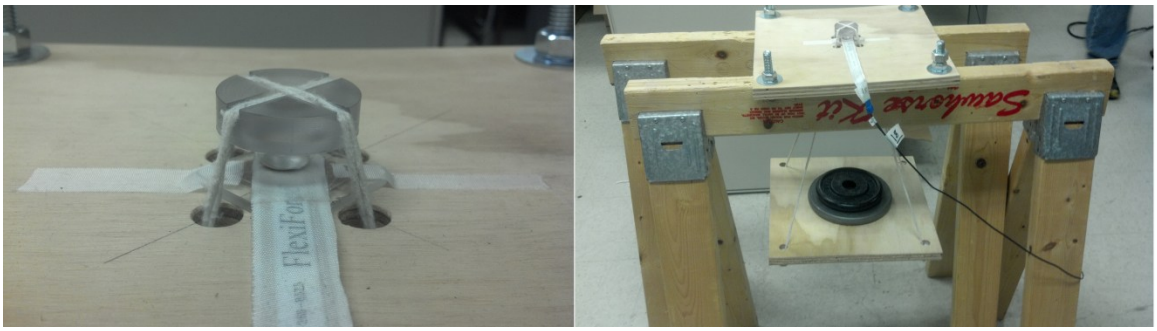

Figure 11: Left –Fixture used to localize force applied. Right – Saw horse calibration method

A second method calibration method involved an arm press with a load cell at the tip of the press. The force read by the load cell was assumed to be the same force applied to the sensing area. The load cell needed to be calibrated prior to the FF calibration with weights. This calibration method can be seen in Figure 12.

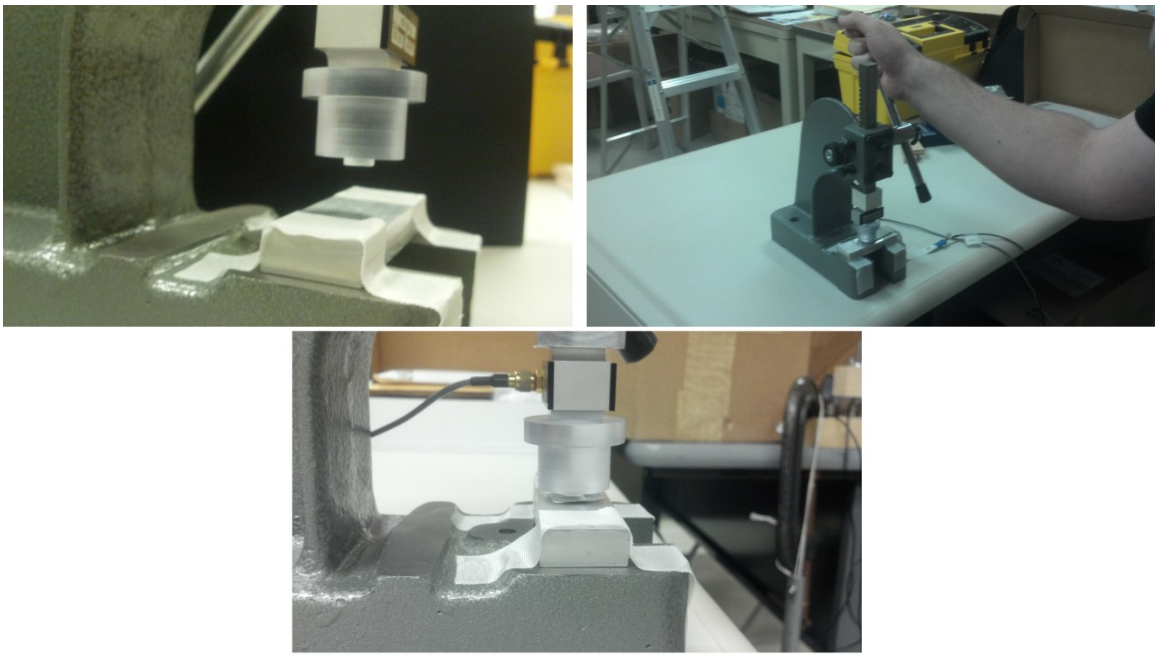

Figure 12: Left - Fixture for localizing force. Right - Arm press. Bottom - Arm press calibration method

These first two methods worked well for lab purposes but were impractical for field use. To be consistent, a method was developed for both lab and field calibrations. In this method, a known force was randomly applied to each FF sensor using a pinch force meter

(PG-30, B&L Engineering, California, USA). The applied ranged from 0 to 20 lbs. in 2.5 lb. increments. During calibration, the sensor is connected to the portable force unit and the peak output voltage is read by a digital multimeter (DMM) for each of the randomly applied forces. A linear best fit is used to relate the force applied by the pinch force to the peak output voltage of the sensor. This was done to convert voltage to pounds force. This calibration method can be seen in Figure 13.

Figure 13: Calibration of a FF sensor using pinch force gauge

2.1.2 Portable Force Unit Construction

Once the circuit design was completed and tested on a protoboard to meet all specifications, the circuit was moved onto a through-hole circuit board and the unit was constructed. Monophone jacks (3.5 mm) were used to connect the sensors to the portable force unit and Bayonet Neill–Concelman (BNC) connectors were used for output connectors to external instrumentation. Due to the way the FF sensors work, the outside terminals of the jacks were connected to the -5 V supply voltage rather than the ground. Alternatively, the outside terminals of the BNC connectors were connected to ground. Initially, this posed a problem due to the shielding of the electronic project box because it was made of a plastic-metal composite that combines metallic electromagnetic shielding with light weight plastic. The connection configuration of the FF and BNC connectors led to a condition where the metal filaments made contact between both connectors and

short circuited the ground on the output side to the -5 V source on the input side. To solve this problem, a special window was constructed to separate the two connectors and avoided these potential shorts. The window can be seen in Figure 14 and the internals of the finished unit in Figure 15.

Figure 14: Side view of the finished unit showing the power button and the custom window made to prevent shorting

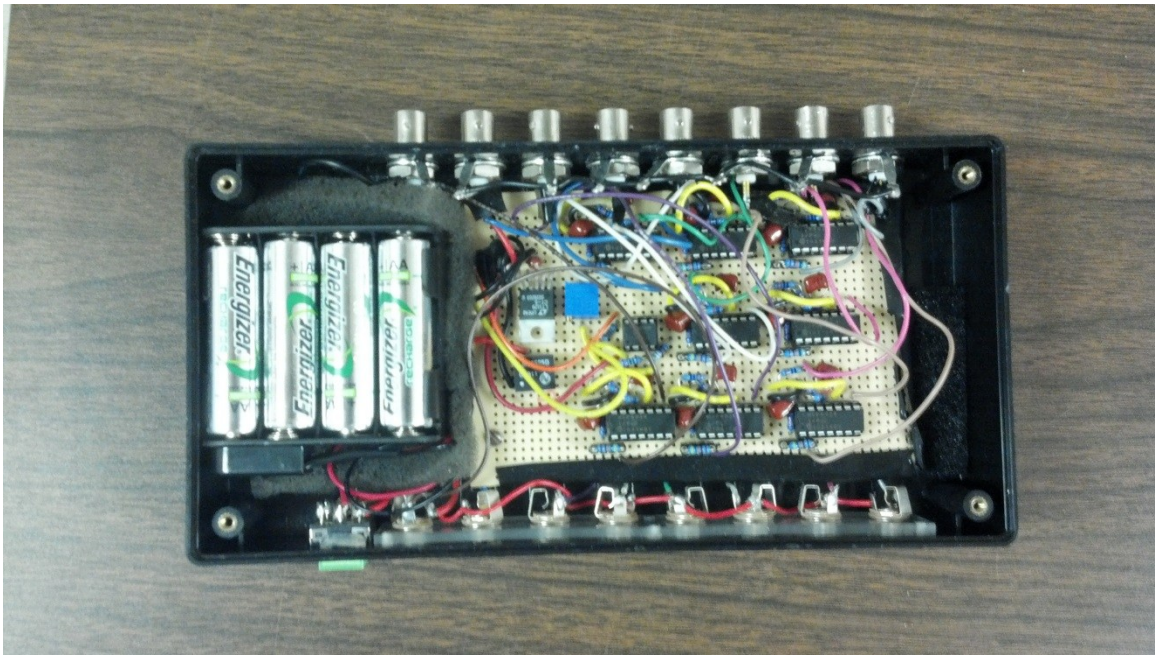

Figure 15: Top view of the finished unit with the cover removed

2.1.3 Data Acquisition Systems

While the FF sensors were powered and conditioned by the custom designed portable force unit, the output of the unit was fed into an ADC (LabJack U12, Lakewood, Colorado, USA). The U12 unit then transferred the data to a computer for storage and processing. Outputs on the force unit were designed so that any ADC, oscilloscope, or dynamic signal analyzer (DSA) can be used to view or capture the output of the sensor signals.

2.1.4 Software

All data collection was done with LABVIEW (National Instruments, Austin, Texas, USA), which was written to incorporate the many different sensor types as well as ADCs being used for calibration, lab use, and field use. The programs managed and collected data from up to three ADCs and various sensor types and allowed for the simultaneous capturing of multiple sensors. For quick visuals of the waveforms,

Acqknowledge (BIOPAC, Goleta, CA, USA) was used, while MATLAB (MathWorks, Natick, MA, USA) was used for post processing and data analysis.

2.1.5 Grip Force Handle

The NIOSH-owned instrumented grip force handle developed by Wimer et al. (2009), discussed in the introduction, was used in this study. A program, supplied by NIOSH, was incorporated into the study and a cable and junction box were developed in order to couple the signals from the handle to the ADC system. The handle has six cantilever beams that measure the normal force applied to each arm and measures 40 mm in diameter and 155 mm in length and can be seen in Figures 16 and 17.

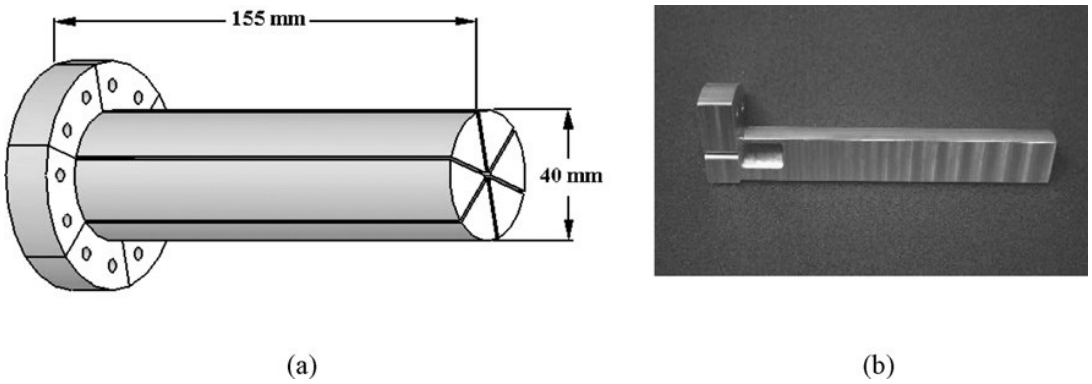

Figure 16: (A) NIOSH Instrumented handle including dimensions and (B) a single measuring beam from the six-arm handle (Wimer et al., 2009)

Figure 17: The experimental set up of the instrumented handle

Wimer et al. showed that the results of the handle are within 4% tolerance if the force is applied at the base or at the tip of the handle and suggested that handle does not correlate well with the traditional Jamar handle, indicating that the Jamar handle may be inadequate for grip force measurements. The instrumented handle uses strain gauges to measure the deflection of the cantilever beams and correlates the deflections and associated strain to the normal force applied to each beam. For calibration, the grip force handle is mounted horizontally and known weights, ranging from 0 to 30 lbs., are randomly chosen and suspended from each beam such that the weight was only distributed on the one arm being calibrated, this can be seen in Figure 18.

Figure 18: The calibration setup of the instrumented handle

The voltage output is recorded for each arm and each weight and a linear best fit is applied. The handle was calibrated routinely and the linear best fits were used to convert the voltage to pounds during testing. The grip force handle used the data acquisition

system that was provided by NIOSH and included an ADC NI 9237 (National Instruments, Austin, Texas, USA) which transferred the data to the computer for storage and processing.

2.2 Laboratory Studies

The first experiment explored the relationship between the force supplied by the thin-film sensors and how it compares to the total grip force provided by the instrumented handle. The goal of this experiment was to understand the minimum number of thin-film force sensors necessary to accurately model total grip force.

For this experiment, only lab personnel working on this project were used as subjects and an IRB was not obtained for this piloting study. Factors such as age, gender, hand anthropometry, and hand dominance were noted. Hand size data were recorded to investigate if smaller hand sizes have less contact area with the handle, and, thus; greater force distribution over the smaller area compared to a subject with a larger hand. If this is true, the conversion factors to model total grip force for subjects with larger hands should have higher values than those subjects with smaller hands, based on thin-film sensor readings. This is due to the fact that the sensors are capturing less of the total force since the sensing area of the sensors is constant.

For this experiment, six trials were run with eight FF sensors taped to the subjects' hands using medical tape for each subject. The trials sequentially moved the FF sensors down the digits and palm to mapping a total of 24 sensor locations of each subject's hand. The first trial had four FF sensors mounted across the distal phalanges (DP) of digits two through five and four FF sensors placed across the palmar aspects of the metacarpophalangeal (MCP) joints of the same digits as seen in Figure 19a. Trials

two and three moved the DP sensors to the pad of the medial phalange (MP), Figure 19b, and proximal phalange (PP), Figure 19c, of the same digits, respectively, while keeping the sensors across the MCP constant. Trial four was identical to trial one, Figure 19d. Trials five and six held the sensors along the DP constant while moving the sensors along the MCP down to map the first digit and palmar aspect of the hand. Trial five mapped below the MCP, in the thenar region, as well as the DP of the first digit, Figure 19e. Trial six mapped the lower palmar aspect of the hand, in the hypothenar region, as well as the proximal phalange of the first digit, Figure 19f. Figure 20 shows the sensor positions with a position identifier. These identifiers are used throughout the study for quick references to sensor positioning.

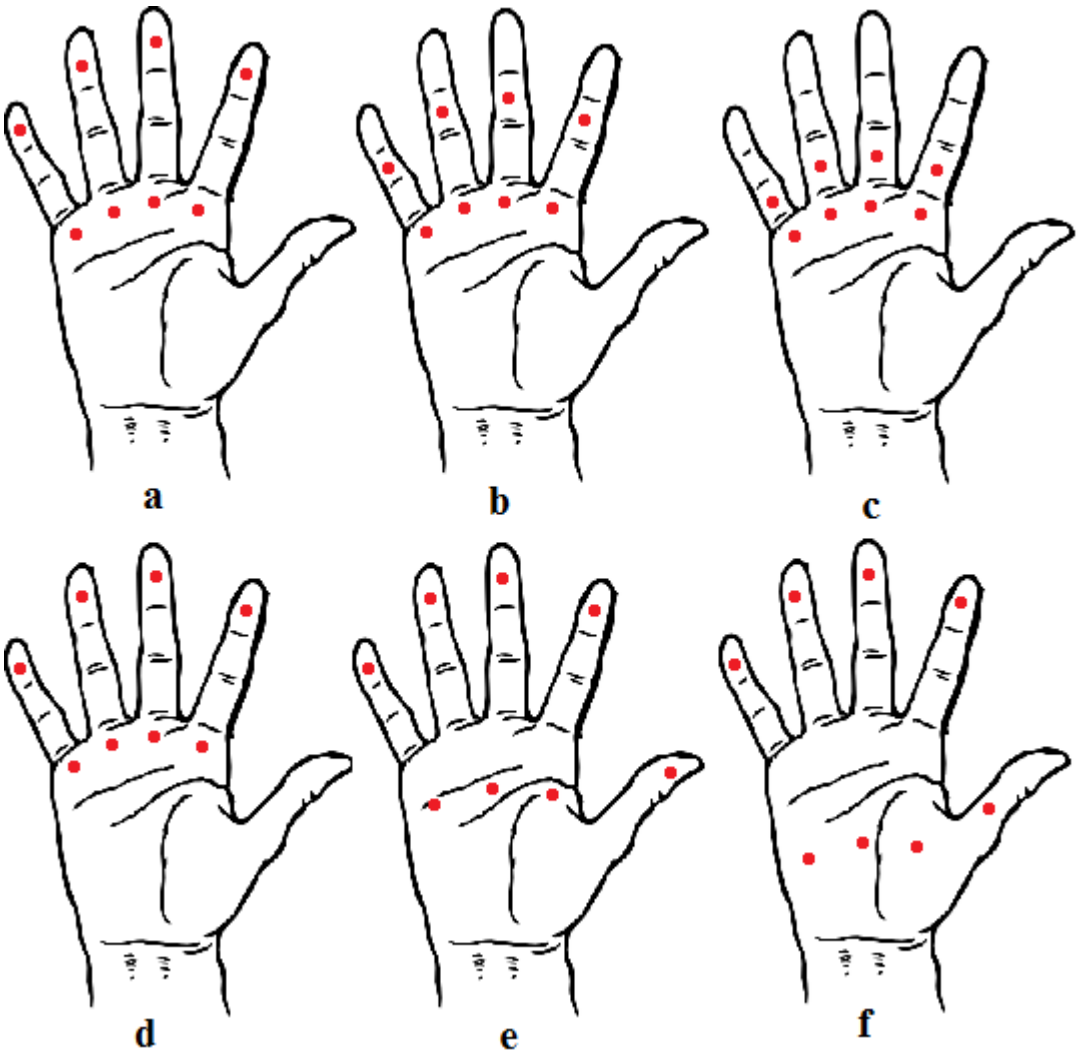

Figure 19: Sensor placements for trials 1 to 6 corresponding to a-f respectively

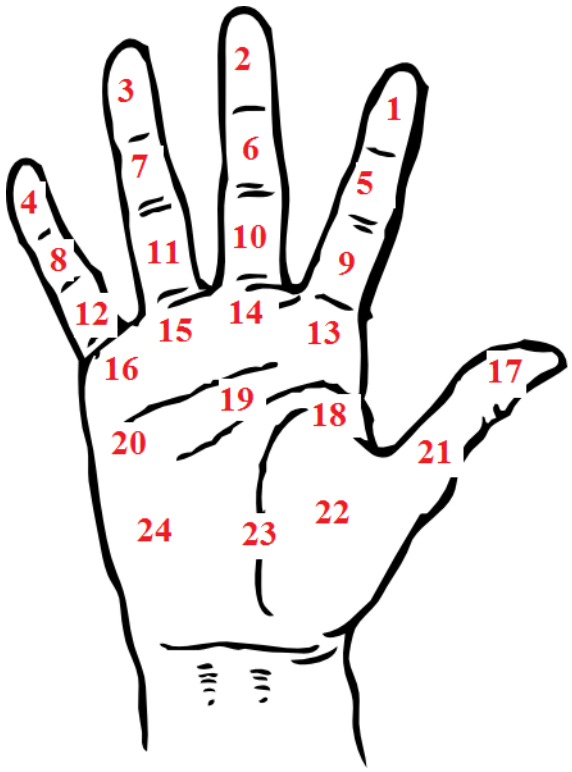

Figure 20: Sensor positions labeled with a numerical indicator for quick reference

When the sensors were placed for each trial, a quick practice test was performed to ensure that the sensors were registering force. Once this was confirmed, the subject was asked to gradually grip up to 80% of their maximum grip. The reason for gradual grasping is to account for the entire curve of the force waveform rather than just plateaus (i.e. individually targeted force levels), giving a more even distribution of values. The value of 80% had been determined prior to testing by having the subject grip the handle without any sensors attached and was selected so that strong force readings could be measured without the effects of fatigue influencing a subject's grip. For each trial, the subject was asked to grip to their target value of 80% three times and, when a trial was complete, the sensors were moved to the next trial's sensor locations.

The force readings were acquired at a rate of 5 Hz. The LabJack ADC was in an on-demand sample mode that synchronized sampling with the NI 9237. Both of these

acquisition systems were integrated into a single program using LABVIEW, which wrote the force output from the two systems data to a single ascii-formatted file.

Once data collection was complete, analysis was performed using MATLAB. A code was written to open the text file and calculate the sum of the six arms for the instrumented grip force handle. This sum was assumed to be the true value and was used as the reference. The program then structures the order of the FF sensors according to sensor response with the highest response first and the sensor with the lowest last. Next, it calculates the sum of all FF sensor waveforms from eight sensors down to one. Each time, it eliminates the sensor with the lowest sensor response leaving the sensors with the best response as the remaining sensors in the summation. Sensor response is determined by the average force reading through the entire trial.

Finally, the program divided the total known grip force, represented by the instrumented handle, by the sum for each combination of FF sensors on a per sample basis according to

$$C(n) = \frac{F_{handle}(n)}{\sum_{i=1}^{I} F_i(n)}, \qquad (7)$$

where C(n) is the conversion factor, F_{handle} is the force represented by the instrumented handle, F_i is the force from the ith FF sensor, and I is the total number of sensors used in the current sensor combination. The ratio between the FF sensors and the handle can be thought of as a conversion factor. The final conversion factor, C_{ave}, was averaged for the entire run, excluding the initial values where no forces were detected. The conversion factor refers to the use of a specified number of sensors in proper locations, where there is a known value that scales the summation of the thin-film sensors to represent the total grip strength according to Equation 8.

$$F_{model}(n) = C_{ave} * \sum_{i=1}^{I} F_i(n), \qquad (8)$$

where $F_{model}(n)$ is the grip force output of the model. The reciprocal of the conversion factor is the percentage of force that the FF sensors represent when directly compared to the total grip force, as given by the instrumented handle. Alternatively, rather than dividing the total grip force by the sums of the FF sensors, it can be divided by each individual FF sensor's force reading to determine the individual sensors conversion factor. This can be thought of as an individual weighting for each sensor and, when combined with other sensors, represents the total grip force.

2.3 Field Measurements

The portable force unit was used in the field as well as in laboratory measurements. Two work sites in which workers regularly use pneumatic power tools were selected for monitoring vibration and grip force data. The subjects studied at these work sites were manufacturing employees who voluntarily agreed to participate in the research. All thirty plus subjects provided their informed consent according to the IRB policies of the University of Connecticut Health Center. Due to time constraints in the field and the work day interruption, hand anthropometry measurements were not taken; however, the type of glove being worn, the subject's handedness, and the tool being used were all documented. Depending on the tool being used, a varying number of FF sensors could be used, which was documented along with pictures to illustrate the grip of each tool.

In general, force measurements were made using the same equipment that was used in the laboratory experiments with the exception of using an alternate data acquisition device for the vibration measurements, which is explained in detail later in

this section. The FF sensors were used as the thin-film sensors, which were powered and conditioned by the portable force unit developed. The signal was then passed into LabJack, which transferred the data to the computer for storage. The instrumented grip force handle was also used in the field for individual subject calibration and to capture the surrogate grip force data. When the handle was not in use and the subject was using a pneumatic power tool, a different ADC was used (Wavebook 512, IOtech, Norton, Massachusetts, USA). The Wavebook was used in order to capture vibration signals, along with tool grip signals, at the higher sampling rates. Figure 21 shows the setup used in the field, where all of the equipment was built into a cart for mobility, with the exception of the instrumented handle, which was mounted on a tripod.

Figure 21: Equipment cart for field use and tripod mounted handle

The capturing process was broken up into three stages. The first stage was considered a calibration process, where the subject was asked to demonstrate how they

grip their tool in order to determine the best FF sensor placement locations. When the locations had been determined, it was documented in the notes and the subject was asked to grasp the instrumented handle and grip from 20 to 100 lbs. force in increments of 20 lbs. in a randomized order. This calibration stage gives a five point relationship between the FF sensors and the grip force handle.

The second stage of capturing consisted of the subject using a pneumatic power tool with the FF sensors placed between the tool and the subject's hand or glove at the locations determined in stage one. It was during this stage of capturing that the Wavebook was used for FF data acquisition, instead of the LabJack, due to the vibration measurements occurring simultaneously. The data was captured for three to five cycles of tool use with an increased sampling rate of 9000 Hz.

The third, and final, stage of capturing required the subject to go back to the grip force handle, with the FF sensors still at the predetermined locations, and grip the instrumented handle at with the same grip force they had just used when operating the pneumatic power tool. This is known as a surrogate grip force measurement and is typically used when direct force measurements are impractical or not possible. The subject was asked to repeat this perceived grip strength three to five times for consistency and to avoid bias. This surrogate measurement was done to explore the relationship between the perceived grip force by the user and the actual grip force during tool use and to investigate the accuracy of the surrogate measures. It should be noted that in all of the field measurements, the FF sensors were loosely placed in the target locations rather than taped, like in laboratory experiments, due to time constraints and the need for subject mobility.

Several analyses can be made from the field measurements. One of the analyses used the calibration stage as a reference for each subject to see how the sensors and handle respond to their grip. This relationship was used to determine a field subject specific conversion factor, which can be applied to the actual tool use waveforms as a model for obtaining total grip force.

The information gathered from the laboratory study was used on the field data to test and observe the accuracy of the selected numbers of sensors used to model the total grip force by either the best sensor response per trial method or by the alternative method of the individual sensor position's conversion factors. Using the second method (i.e. individual sensor position conversion factors), allows for custom conversion factors for all sensor position combinations with the field data. This is important as it is rare that two subjects used the exact same grip in the field. An expansion of the second method involves the subject sensor positions from the field that have already been collected for different tools and different grip types. In this thesis, there are three categories of interest investigated: pistol grip, in-line straight grip, and bucking bar grip. Using the individual sensor position's conversion factors, category templates can be made to be applied to future field investigations.

3. Results

3.1 Portable Force Unit

The portable force unit was successfully designed and constructed in the laboratory and contains eight channels to power and condition eight FF sensors. Before being implemented in the field or in laboratory experiments, several tests were completed to validate its application. The first test performed validated the expected current draw for the unit. For the operational amplifier (op-amp) chosen, the current draw is roughly 5 mA from a +5 V single supply rail, giving a current draw of 40 mA for the op-amps alone for all eight channels. The expected current draw is close to 50 mA, with the additional 10 mA from the low battery circuit components and sensor power. When tested, the actual current draw of the circuit was 48.6 mA, indicating that there were no shorts between power and ground.

A battery test was run to see how long the unit could operate using eight rechargeable 2300 mAh batteries. The low voltage dropout for the regulator is 6.5 V and the low battery circuit was set to turn off the indicator at 7.5 V to signal a low battery condition. The test recorded how long it takes for the battery power to decrease from a fully charged 10 V down to 5 V. As mentioned in the methods, the minimum requirement was that the unit needed to be powered for eight hours or for a full work day cycle. The battery voltage was sampled once per minute until the battery voltage reached 5 V and the results of the test can be seen in Figure 22. The unit far surpassed its requirements, lasting over 40 hours before the battery life started to decay, which is more than five times the specification requirement of eight hours.

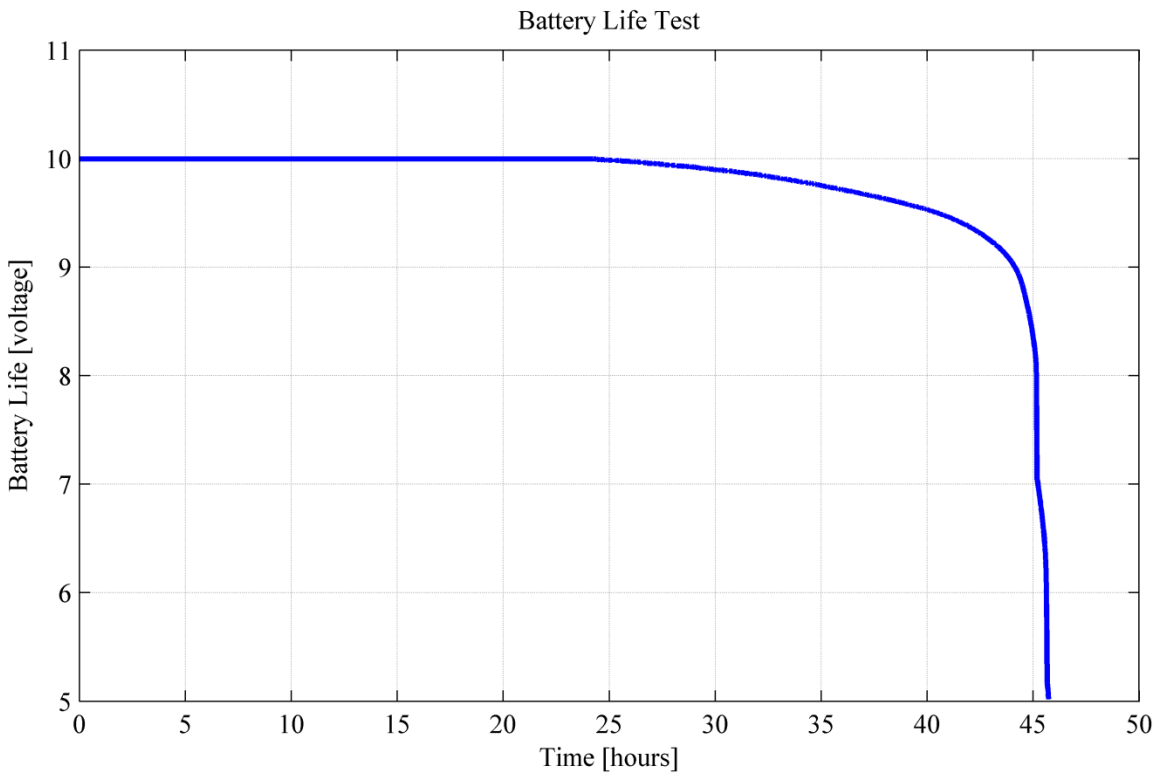

Figure 22: Battery life test

Validation of the filter in the second stage of the circuit was done using a frequency response test on a Dynamic Signal Analyzer (DSA) (Model SR785, Standard Research Systems (SRS), Sunnyvale, California, USA). The frequency response was run using a swept sine that started at 5 Hz and ran up to 2000 Hz; however, due to the way the sensor works, the first stage of the circuit, the amplification stage, could not be included in the frequency response because the sensor changes resistance and not voltage. As a result of the sensor characteristics, passing the voltage input from the DSA through the amplification stage to simulate the sensor does not accurately represent the circuit frequency response. Instead, the signal was introduced at the beginning of the filter stage and the output was recorded after the buffer. Figure 23 shows the theoretical filter frequency response simulated in MATLAB in gray and the actual measured filter response from the DSA in black.

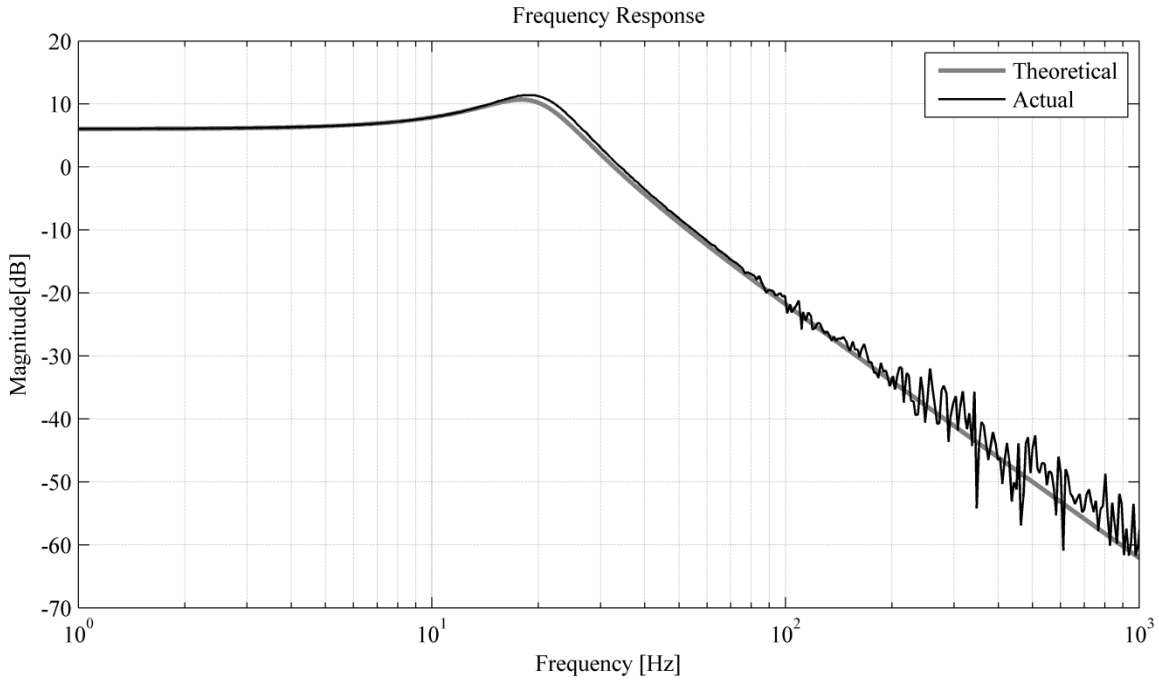

Figure 23: Frequency response test

Noise interferes with the ability of the circuit to accurately represent a certain sensor input and therefore it is important to understand the noise levels of a system. Four baseline noise measurements were taken at a sampling rate of 4000 Hz. For these tests, a FlexiForce sensor was connected to four different channels and left flat on a table with no input force on the sensing area. The root-mean-square voltage (Vrms) was acquired for the entirety of the capture time, which was about 90 seconds. The peak-to-peak voltage (Vpp) values were averaged together from the four trials. The average Vrms noise level was 0.7 mV and the average Vpp value was 8.9 mV. The Vpp noise corresponds to roughly seven analog-to-digital conversion steps on the 12-bit data acquisition system.

An example calibration is shown in Table 1 to demonstrate the dynamic range of the force sensor unit with the forces applied and the corresponding voltages. The calibration was carried out in the manner explained in Section 2.1.1.

Table 1: An example calibration using a multimeter

Applied Force [lbs.]	Voltage [V]
0	0.0143
2.5	0.1473
5	0.2478
7.5	0.3695
10	0.5267
12.5	0.633
15	0.7533
17.5	0.8666
20	1.0114

This calibration gives a slope and intercept of 0.04947 and 0.01305 respectively. When using this linear fit and solving for a 100 lb. force the voltage would be 4.96 V. This meets the desired force input range specification to accept forces from 0 to 100 lbs. as long as the ADC is set to at least an input voltage range of 0 to 5 V.

The demonstrated tests prove that the unit meets all of its design specifications by exceeding the battery life requirement, amplifying and filtering up to eight sensors at once, and showing that the correct amplification and filtering has been designed to maximize resolution and minimize noise during the collection process.

3.2 Laboratory Experiments

The gender, handedness, age, and hand anthropometry of the seven subjects are presented in Table 2.

Table 2: Summary of subjects hand anthropometry, age, gender, and hand dominance. (Length measurements in cm)

Subject	1	2	3	4	5	6	7	Ave	St.Dev
Gender	F	M	M	F	F	M	M	N/A	N/A
Hand Dominance	R	R	R	R	R	R	R	N/A	N/A
Age (yrs.)	20	21	24	19	21	24	25	22.1	2.19
Thumb (Length)	11.2	11.0	11.5	9.6	9.8	10.4	11.3	10.7	0.76
Thumb (Width)	1.9	2.0	2.3	1.9	1.9	2.3	2.5	2.1	0.25
Index Length	7.9	6.7	7.8	6.6	6.4	7.6	7.7	7.2	0.64
Index Width	1.8	2.2	2.0	1.7	1.8	2.1	2.2	2.0	0.21
Middle Length	8.8	7.4	9.1	7.1	7.1	8.4	8.5	8.1	0.84
Middle Width	1.8	2.1	2.1	1.7	1.9	2.0	2.3	2.0	0.20
Ring Length	8.0	6.9	8.3	6.5	6.7	8.1	7.7	7.5	0.74
Ring Width	1.7	2.0	1.9	1.6	1.8	2.0	2.2	1.9	0.20
Pinky Length	6.5	5.5	6.3	5.0	5.6	6.5	6.8	6.0	0.66
Pinky Width	1.6	1.8	1.7	1.4	1.6	2.0	1.9	1.7	0.20
Palm Length	10.5	10.3	11.0	9.6	9.4	10.2	11.5	10.4	0.74
Palm Width	8.5	8.4	8.8	7.4	7.8	9.0	9.7	8.5	0.76
Hand Length	19.4	18.1	20.0	16.8	16.5	18.4	20.5	18.5	1.53
Estimated Area (cm^2)	164.9	152.0	175.0	124.3	128.7	165.6	198.9	158.5	26.11

The estimated hand area was computed by hand length times hand breadth (i.e. width), which was adopted from Seo et al. (2008). Comparative hand anthropometry measurements were taken from Kodak's Ergonomic Design for People at Work (Chengalur et al., 2004) and can be seen in Table 3. The data in this textbook are from three studies: Champney 1979, Muller-Borer 1981, and NASA 1978.

Table 3: Hand anthropometry for males and females with given percentiles of the population. (Units in cm) (Chengalur, 2004)

Measurement	Males		Females		Population Percentiles, 50/50 Males/Females		
	50th percentile	± 1 S.D	50th percentile	± 1 S.D	5th	50th	95th
HAND							
28. Hand thickness, metacarpal III	3.3	0.2	2.8	0.2	2.7	3.0	3.6
29. Hand length	19.0	1.0	18.4	1.0	17.0	18.7	20.4
30. Digit two length	7.5	0.7	6.9	0.8	5.8	7.2	8.5
31. Hand breadth	8.7	0.5	7.7	0.5	7.0	8.2	9.3
32. Digit one length	12.7	1.1	11.0	1.0	9.7	11.8	14.2
33. Breadth of digit one interphalangeal joint	2.3	0.1	1.9	0.1	1.8	2.1	2.5
34. Breadth of digit three interphalangeal joint	1.8	0.1	1.5	0.1	1.4	1.7	2.0
35. Grip breadth, inside diameter	4.9	0.6	4.3	0.3	3.8	4.5	5.7
36. Hand spread, digit one to digit two, first phalangeal joint	12.4	2.4	9.9	1.7	7.5	10.9	15.5
37. Hand spread, digit one to digit two, second phalangeal joint	10.5	1.7	8.1	1.7	5.9	9.3	12.7

Performing the same estimated hand area measurement taken from Seo et al. (2008) using the data from Chengalur (2004) gives the estimated hand areas seen in Table 4.

Table 4: Estimated hand area based on calculations from Seo et al. (2008) and the population percentiles from Chengalur (2004)

	Males		Females		Population % 50/50		
	50th	±1 S.D.	50th	±1 S.D	5^{th}	50^{th}	95^{th}
Hand length	19.08	1.08	18.48	1.08	17.08	18.78	20.48
Hand breadth	8.78	0.58	7.78	0.58	7.08	8.28	9.38
Estimated Area	167.52	21.18	143.77	19.75	120.93	155.50	192.10

By comparing the estimated hand area of the subjects for this study with the results of Chengalur, each lab subject can be categorized into a small, medium, or large hand size category. Subjects four and five were placed in the small hand size category, while subjects one, two, and six were identified with medium hand size and subjects three and seven with large hand sizes. The role of hand size was investigated from the data

collected to determine if larger hand sizes, with more contact area, capture less force from the FF sensors of fixed size. This is explained in further detail in Section 6.

The DP trial of Subject 2 is presented in Figure 24, where the output of the NIOSH instrumented handle is the black dotted line plotted with the left Y-axis and the different combinations of the varying FF sums are plotted with the right Y-axis. The manner in which a FF sensor was eliminated from the summation each time was by measured sensor response and was determined by the average force reading of the entire trial. This leaves the sensors with the highest contact force readings in the summations until they have the lowest values of the remaining sensors.

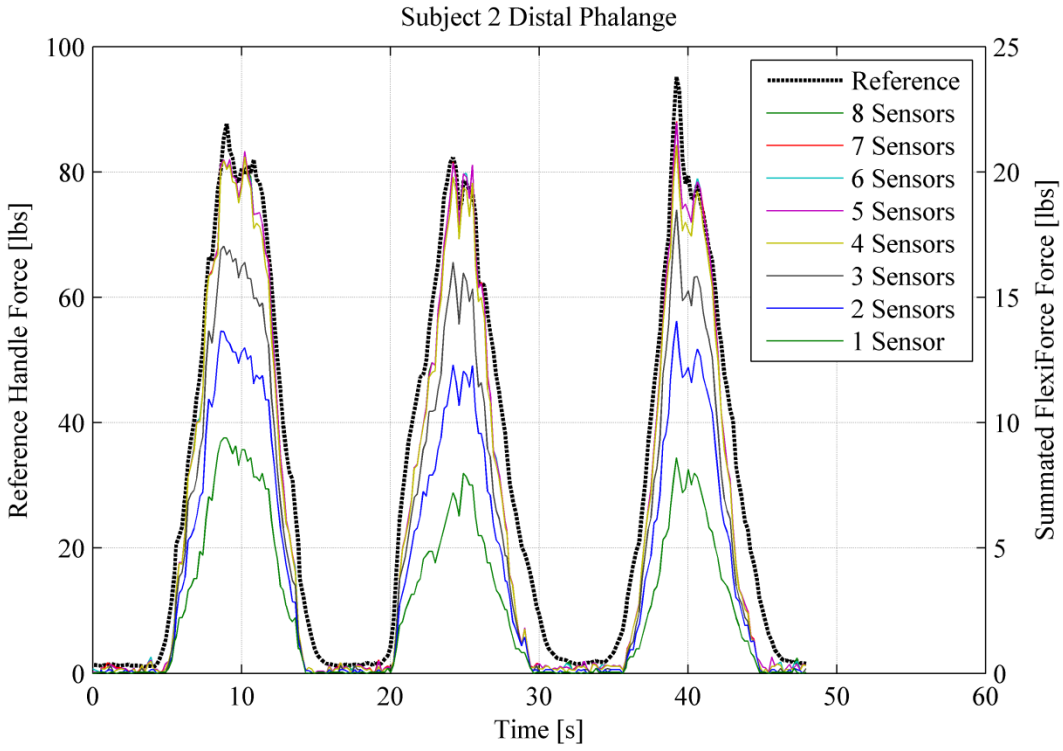

Figure 24: DP trial of Subject 2

Note that if the lines overlapped exactly, then the conversion factor would be four to match the scaling from the left Y-axis to the right Y-axis. To obtain the conversion factor in Figure 24, each of the FF sums were divided into the reference handle's force

while taking into account the scaling difference between the two Y-axis. After this was done for each sample, the trial was averaged for the entirety of the waveform and provided a conversion factor for each of the number of sensors used. This process was done for each subject and trial. The first three trials mapped the fingers with the distal, medial, and proximal phalanges, respectively, while the last three trials mapped the palm with the metacarpophalangeal joint, thenar region, and hypothenar region of the palm. The graphical representations of the conversion factors for each subject for all six trials are shown in Figures 25 through 31.

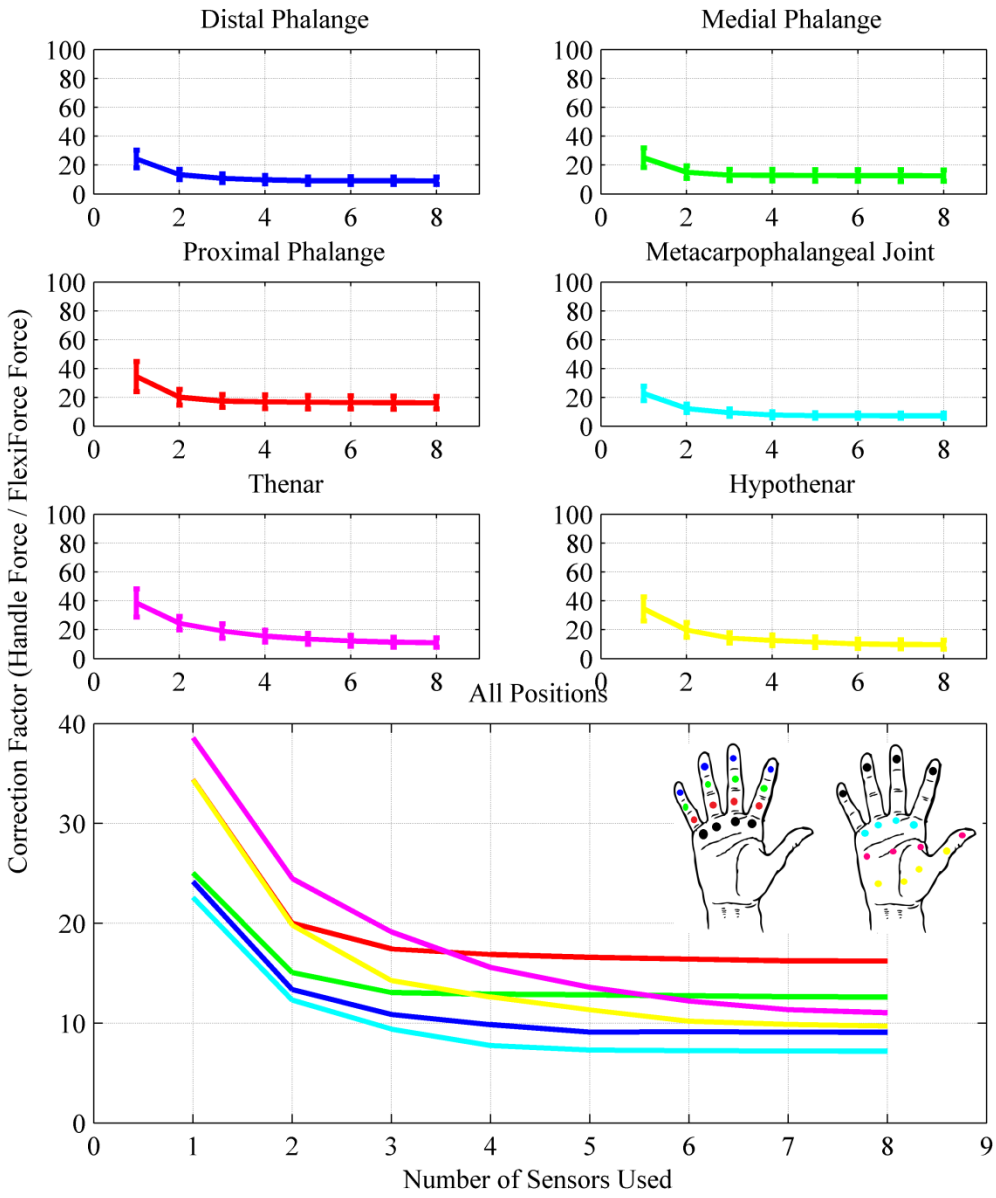

Figure 25: Conversion factors for each of the six trials for Subject 1 shown on the Y-axes and the varying number of sensors used on the X-axes. The last plot is of all trials together without the standard deviation error bars. Black circles in the hand diagram indicate those positions were held constant

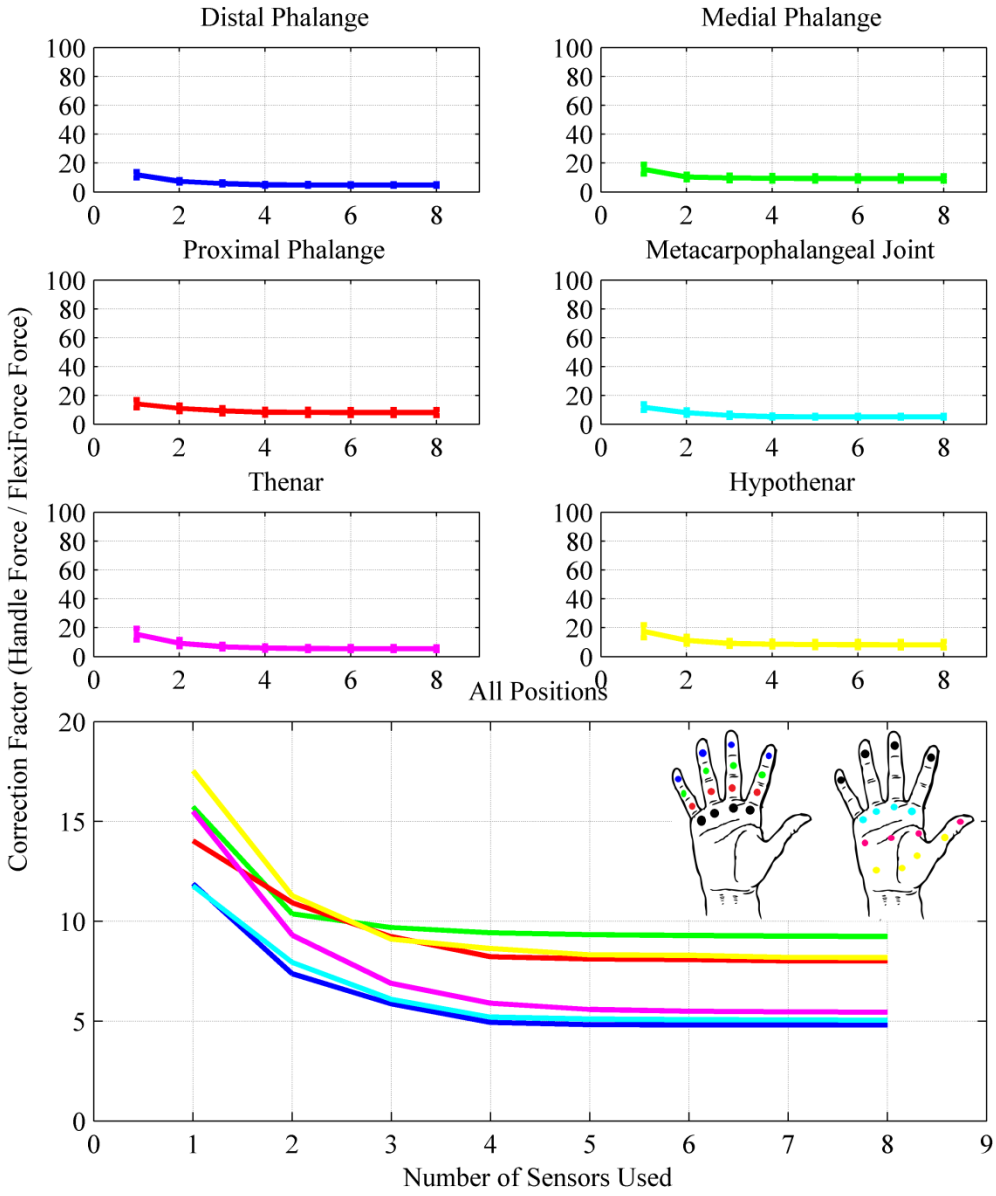

Figure 26: Conversion factors for each of the six trials for Subject 2 shown on the Y-axes and the varying number of sensors used on the X-axes. The last plot is of all trials together without the standard deviation error bars. Black circles in the hand diagram indicate those positions were held constant

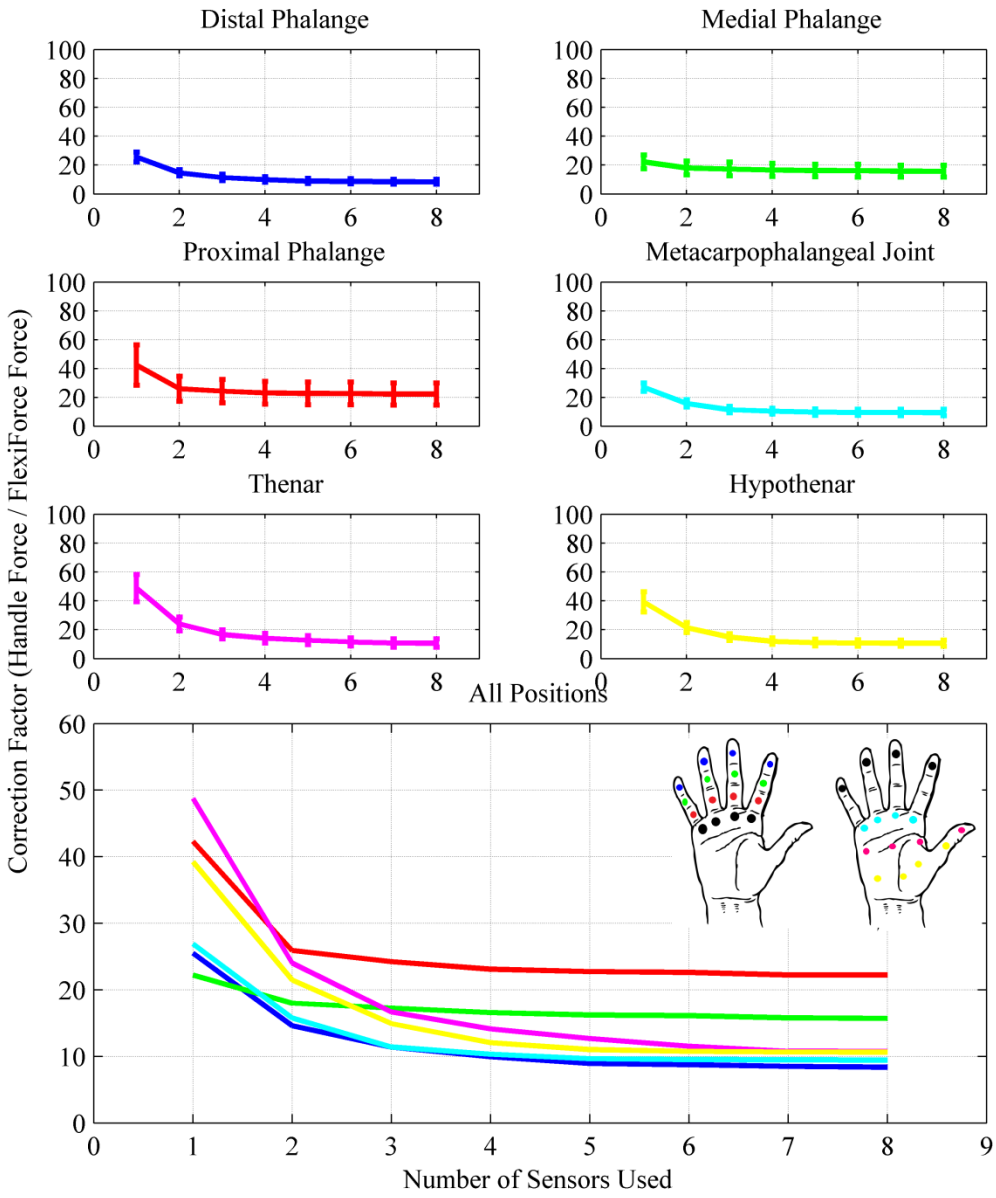

Figure 27: Conversion factors for each of the six trials for Subject 3 shown on the Y-axes and the varying number of sensors used on the X-axes. The last plot is of all trials together without the standard deviation error bars. Black circles in the hand diagram indicate those positions were held constant

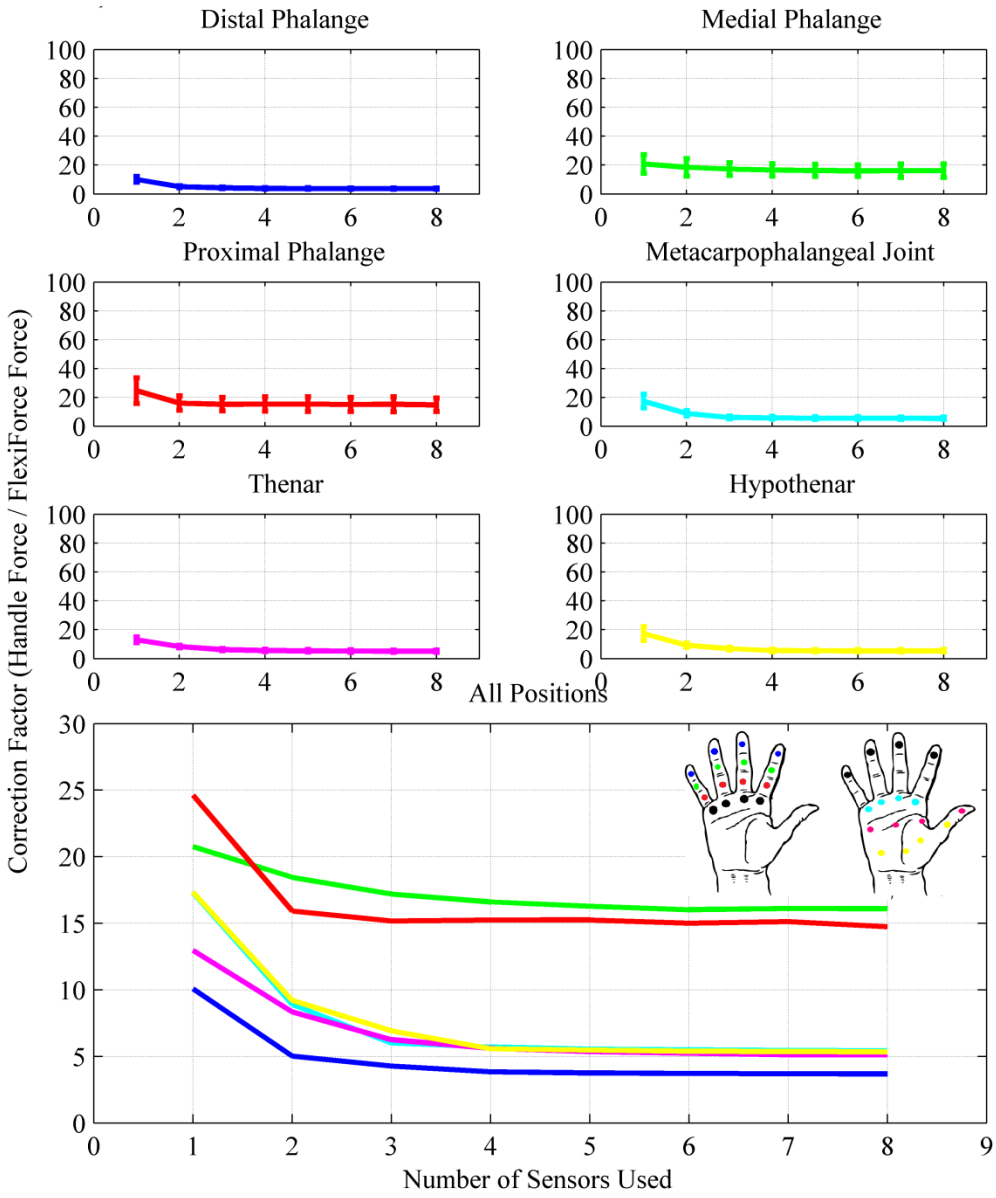

Figure 28: Conversion factors for each of the six trials for Subject 4 shown on the Y-axes and the varying number of sensors used on the X-axes. The last plot is of all trials together without the standard deviation error bars. Black circles in the hand diagram indicate those positions were held constant

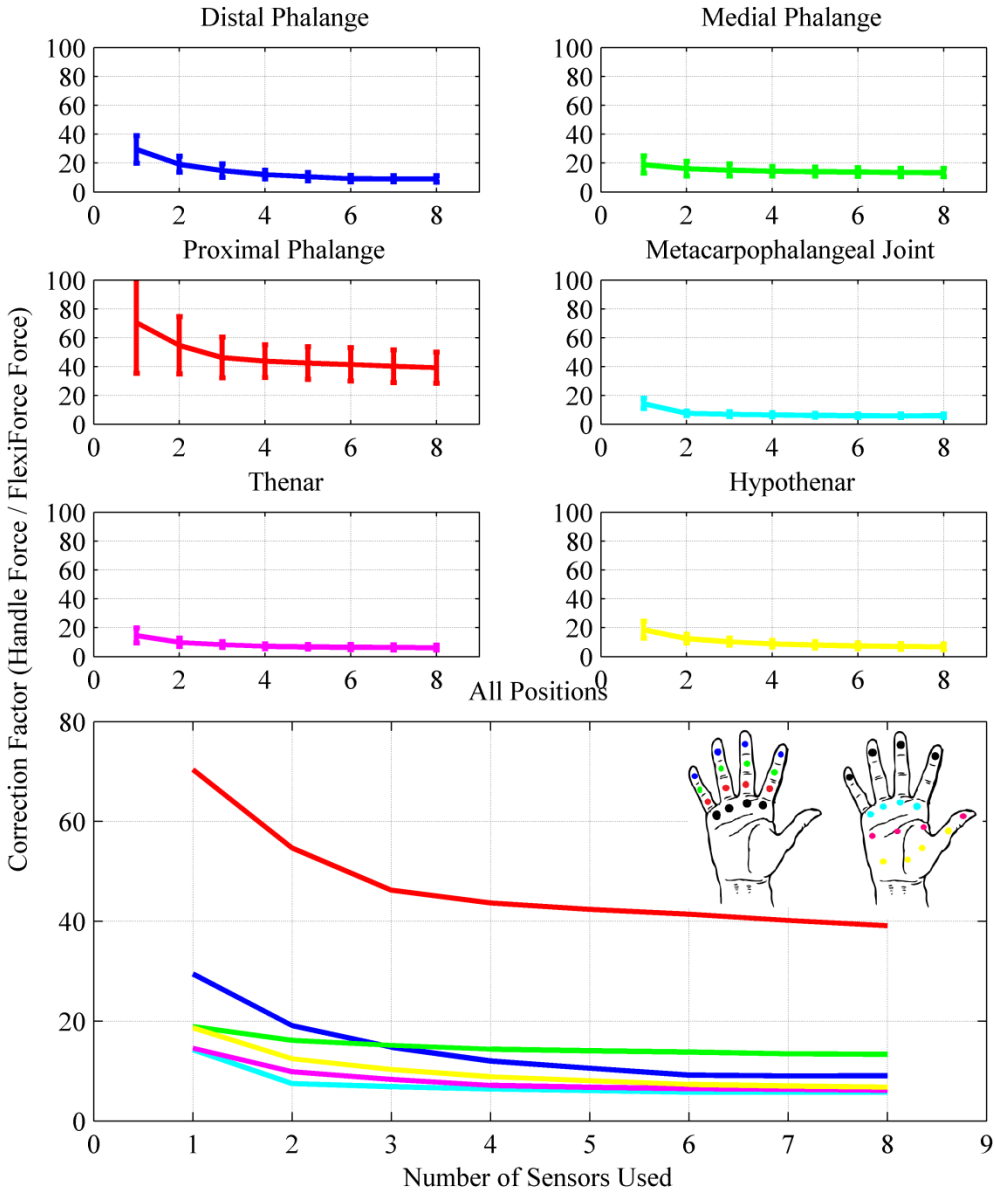

Figure 29: Conversion factors for each of the six trials for Subject 5 shown on the Y-axes and the varying number of sensors used on the X-axes. The last plot is of all trials together without the standard deviation error bars. Black circles in the hand diagram indicate those positions were held constant

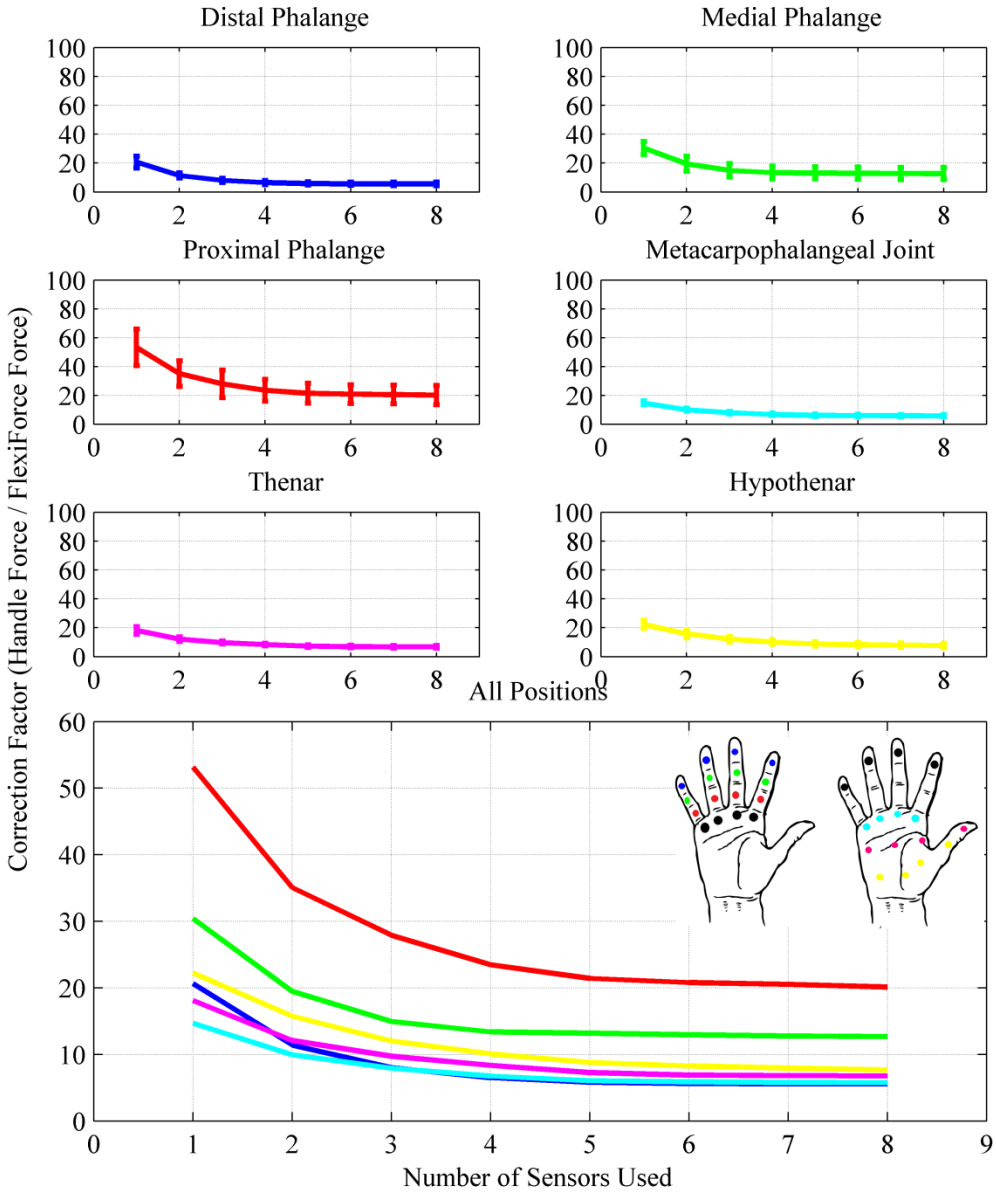

Figure 30: Conversion factors for each of the six trials for Subject 6 shown on the Y-axes and the varying number of sensors used on the X-axes. The last plot is of all trials together without the standard deviation error bars. Black circles in the hand diagram indicate those positions were held constant

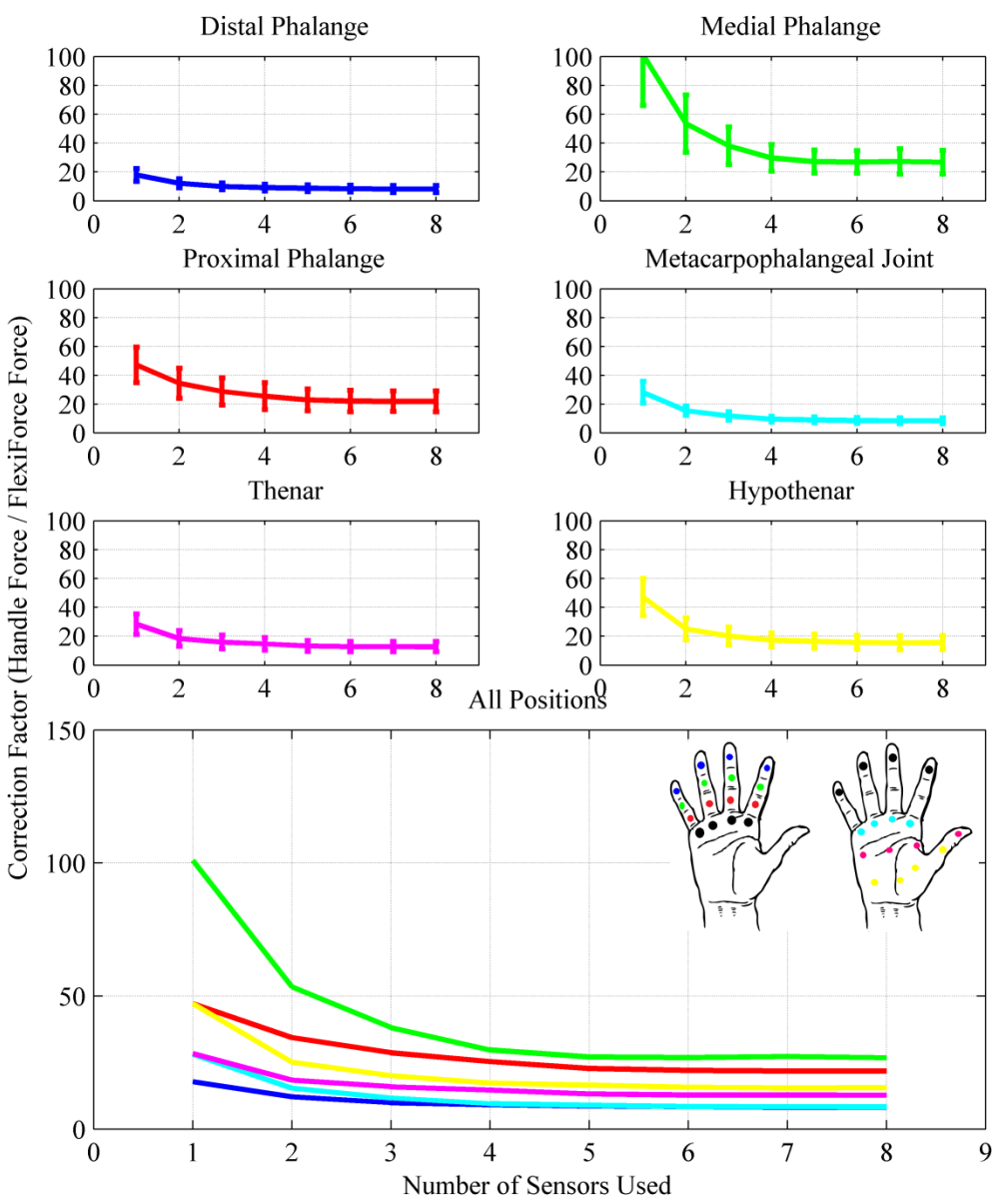

Figure 31: Conversion factors for each of the six trials for Subject 7 shown on the Y-axes and the varying number of sensors used on the X-axes. The last plot is of all trials together without the standard deviation error bars. Black circles in the hand diagram indicate those positions were held constant

When all of the subjects are averaged together, a better comparison can be made between each position and this is displayed in Figure 32.

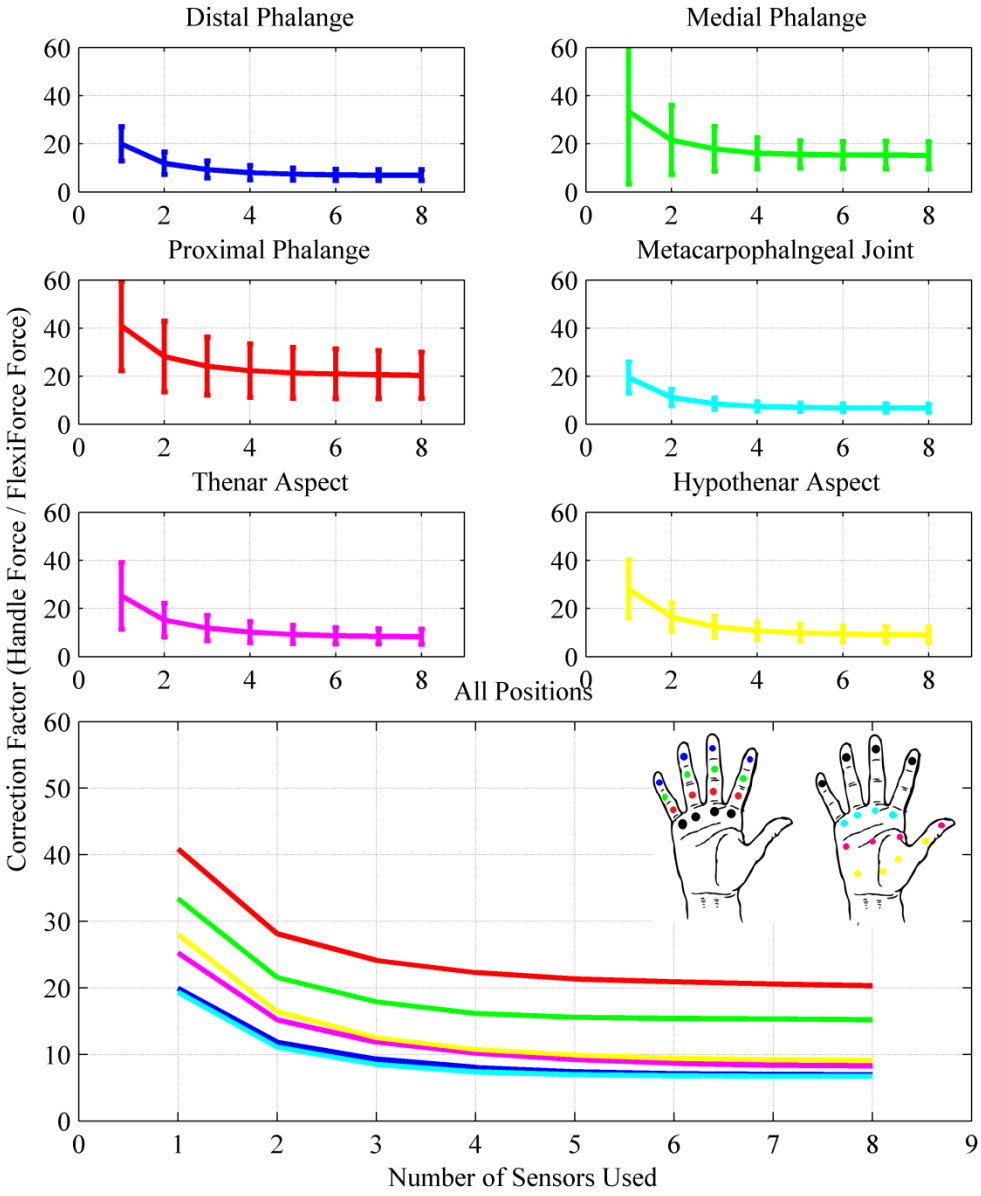

Figure 32: The conversion factors of all positions of all subjects on the Y-axes with the varying number of sensors used on the X-axes. Black circles in the hand diagram indicate those positions were held constant

The conversion factor results can also be represented with respect to each subject in table form by averaging together all of the positions trials for each subject to form one conversion factor per subject for each number of sensors used (Table 5).

Table 5: Conversion factors for each subject based on the number of sensors used

Subject	# of Sensors							
	8	7	6	5	4	3	2	1
1	10.98	11.07	11.33	11.79	12.6	14.03	17.51	29.86
2	6.79	6.8	6.84	6.88	7.05	7.81	9.53	14.41
3	12.86	12.91	13.23	13.55	14.37	15.98	19.96	34.16
4	8.4	8.48	8.48	8.61	8.77	9.31	10.98	17.17
5	13.38	13.63	14.01	14.66	15.41	16.94	19.96	27.71
6	9.76	9.9	10.07	10.42	11.42	13.42	17.29	26.54
7	15.56	15.64	15.72	16.21	17.62	20.73	26.45	44.89
Average	11.11	11.21	11.38	11.73	12.46	14.03	17.38	27.82
St. Dev.	3.05	3.08	3.16	3.34	3.72	4.45	5.75	10.25

In Table 5, the standard deviations remain low until just one sensor was used and the averages showed that, from eight sensors to four sensors used, there was little difference in the conversion factor. When using one or two sensors, however, there was a significant change in the conversion factor. Because of the variation in grip distribution among several subjects, it is important to understand how much of a role hand size plays in the determination of the conversion factors. (Recall that subjects four and five have the smallest hand size, subjects three and seven have the largest, and subjects one, two, and six have medium hand sizes.) Table 6 shows the averaging of the conversion factors according to hand size.

Table 6: Conversion factors for each hand size based on the number of sensors used

Hand Size	# of Sensors							
	8	7	6	5	4	3	2	1
Small	10.89	11.06	11.25	11.64	12.09	13.13	15.47	22.44
Medium	9.18	9.26	9.41	9.7	10.36	11.75	14.78	23.6
Large	14.21	14.28	14.48	14.88	16	18.36	23.21	39.53

In addition to the conversion factors that have been determined, force distribution patterns across the hand were discernible by averaging together the force from each sensor, in each trial, from each subject. The distribution patterns can be seen in Figure 33. For each trial, the sum of the force distribution percentages is 100% and comparisons cannot accurately be made amongst the trials as the forces for both the FF sensors and the NIOSH instrumented handle were not identical between trials.

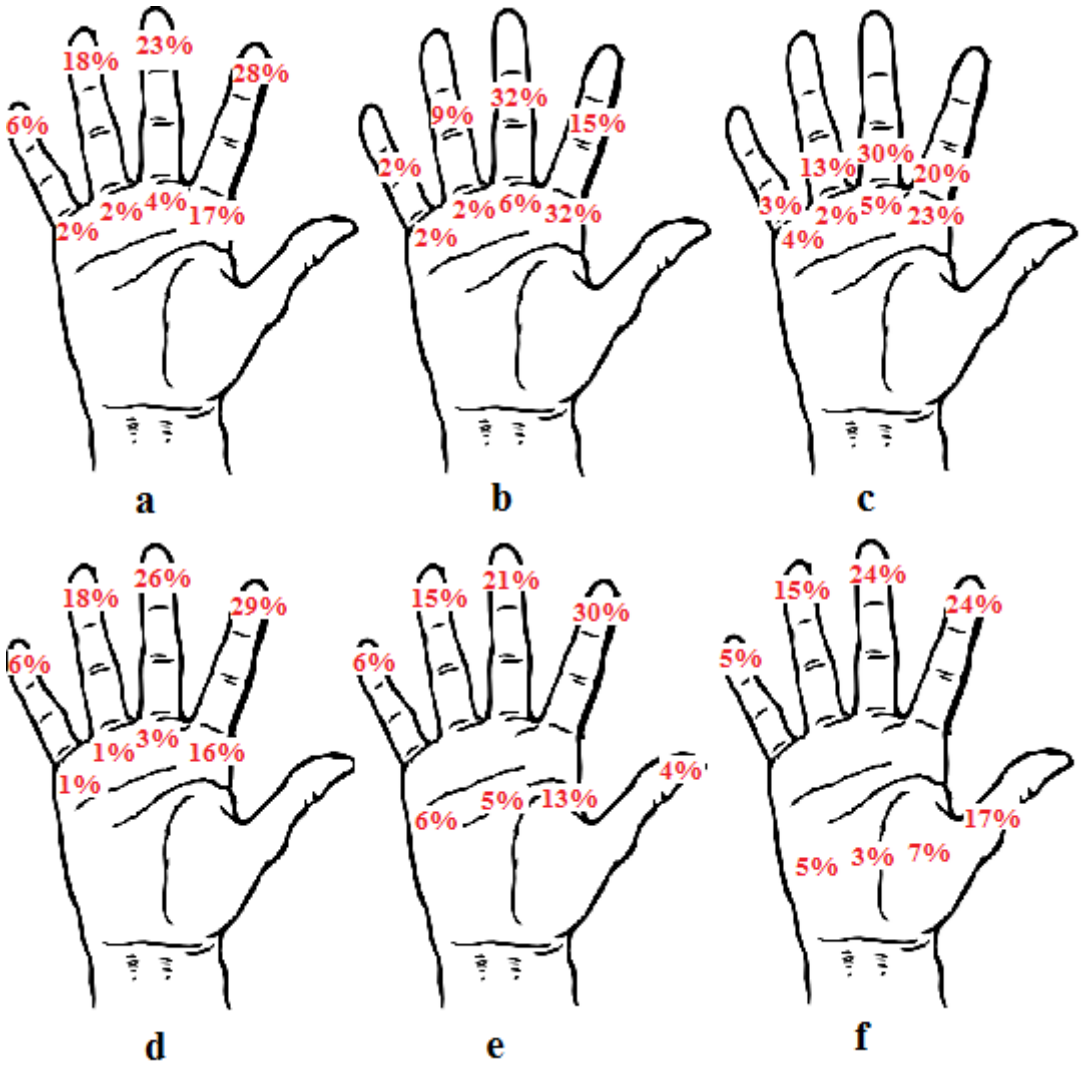

Figure 33: Force distribution pattern for each of the six trials (a-f)

To test the capabilities of this calibration model, several of the subjects have performed additional trials that were not used for calculating the conversion factors.

These additional trials serve as a test data set to determine how accurate the model can be in representing the total grip force, given the number of thin-film sensors used. Figure 34 shows one of the trials (DP locations) and the predicted force values using the models: subject conversion factor model by averaging all of this subject's trials together (Subject CF), position conversion factor model by averaging all of the subjects together for this position trial (Position CF), subject and position conversion factor model by using the data for this subject in this position (Subj. and Pos. CF), and the overall average model by averaging all subjects and all positions together (Overall Average CF). As expected, the subject and position specific conversion factor model is the most accurate since it is based on this subject in this position. The subject model and the overall model overestimate, which is likely due to the fact that the DP has the lowest conversion factors and averaging in the other positions with higher conversion factors, the models overestimate. The position model fits well but not as well as the subject and position model.

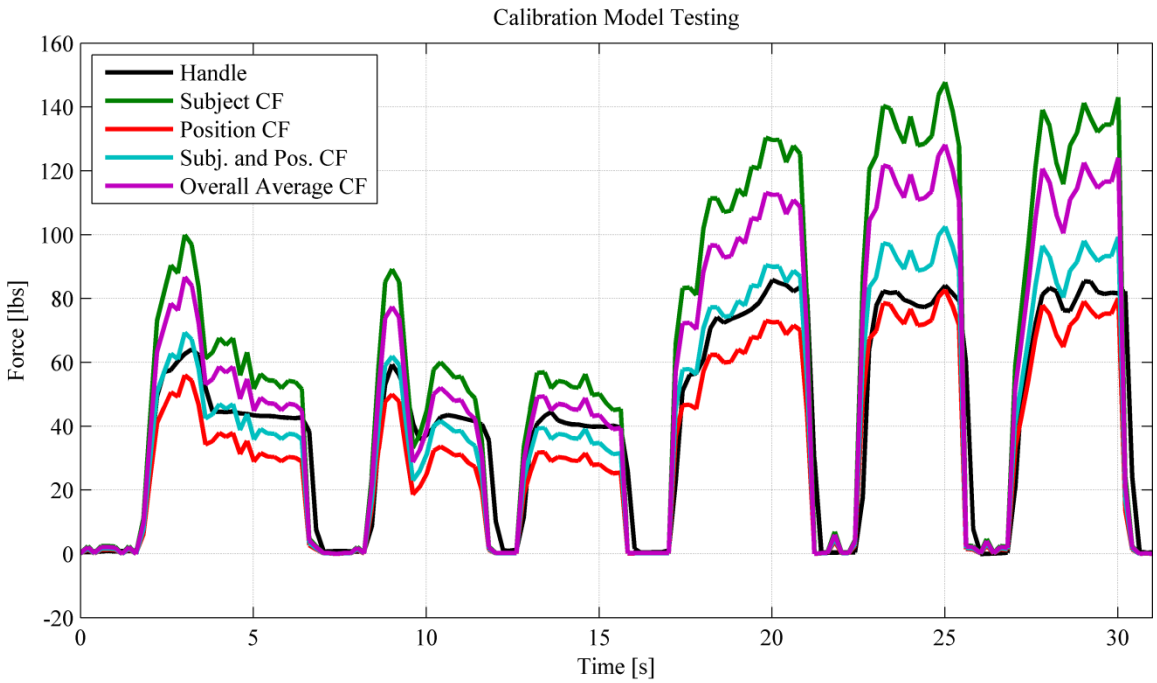

Figure 34: Accuracy of the different conversion factor models developed (Handle is in black, subject conversion factor (green), position conversion factor (red), subject and position conversion factor (light blue), and the overall average conversion factor (purple))

3.3 Field Measurement Results

With force measurements from over 30 subjects in the field, five were selected to apply the calibration models developed in the laboratory, identified as subjects A through E in this thesis. An example of field data calibration is shown in Figure 35 and a sample of the corresponding tool use is shown in Figure 36 for one subject, who used a rivet gun and did not wear gloves.

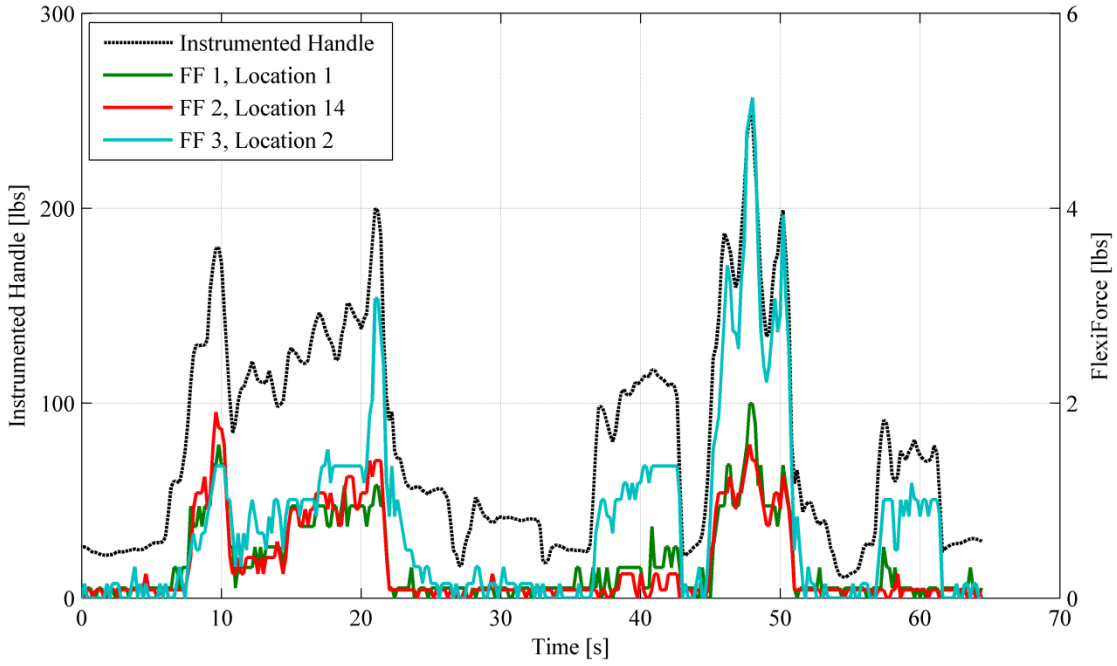

Figure 35: Calibration file for Subject C (The instrumented handle's force, dotted black line, is plotted with the left Y-axis and the three FlexiForce sensors are plotted on the right Y-axis. The sensor locations correspond to Figure 20)

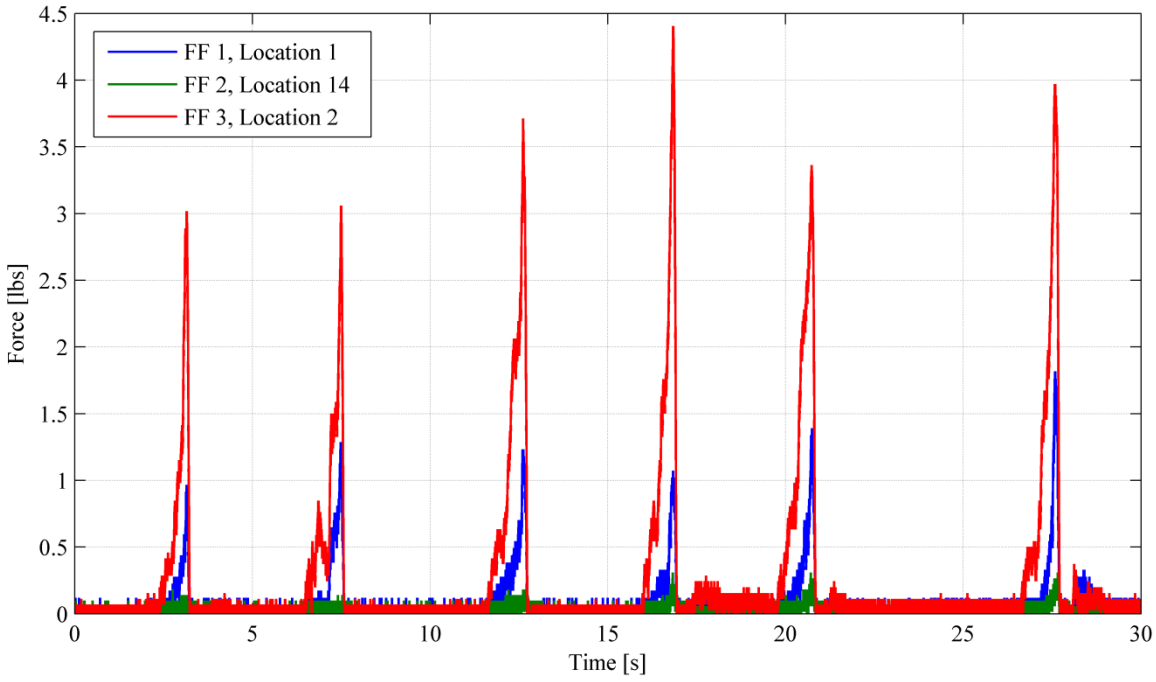

Figure 36: Sample tool use for Subject C (The sensor locations correspond to Figure 20)

Following the same analysis done for the laboratory experiments on the calibration files from the field, a subject specific conversion factor was calculated. It is

important to note that there is a protocol difference between the two calibration processes of the lab and the field. In the lab, the subjects were asked to repeatedly grip at roughly 80% of their maximum grip at a gradual rate, while in the field, the subjects were given five randomized target grip forces from 20 to 100 lbs., in 20 lb. increments. Once the subject specific calibration factor was determined, it was implemented to calculate the total grip force applied during the tool measurement. The process mentioned is presented for five of the subjects and tools studied in the field, one of which is Subject C, whose calibration and sample tool data are presented above in Figures 35 and 36.

Table 7 summarizes the conversion factors used for subjects A through E and Figures 37 through 41 are the graphs for subjects A through E tool use with three models of conversion factors applied to the four, three, two, and one sensor conditions. In the figures, the three models are the field subject calibration conversion factor (Field), the conversion factors for the lab trial that had the sensor positions most similar to that of the field sensor positions (Lab Position), and the overall lab model by averaging all positions and all subjects (Lab Overall). The surrogate measurement (Surrogate) was used as a comparison in each of the subjects presented by averaging the peaks of the surrogate measurements together and plotting the average as a horizontal black line. The surrogate measurement was the level of grip force the subject grasped the instrumented handle with after their tool, trying to simulate the force used on the tool.

Table 7: Field calibration conversion factors for each subject

Subject	Number of Sensors			
	4	3	2	1
A	11.79	12.09	14.05	16.76
B	18.81	19.96	20.58	38.15
C	24.87	25.11	32.93	47.09
D	15.18	15.57	23.03	38.6
E	8.18	8.26	10.25	17.27

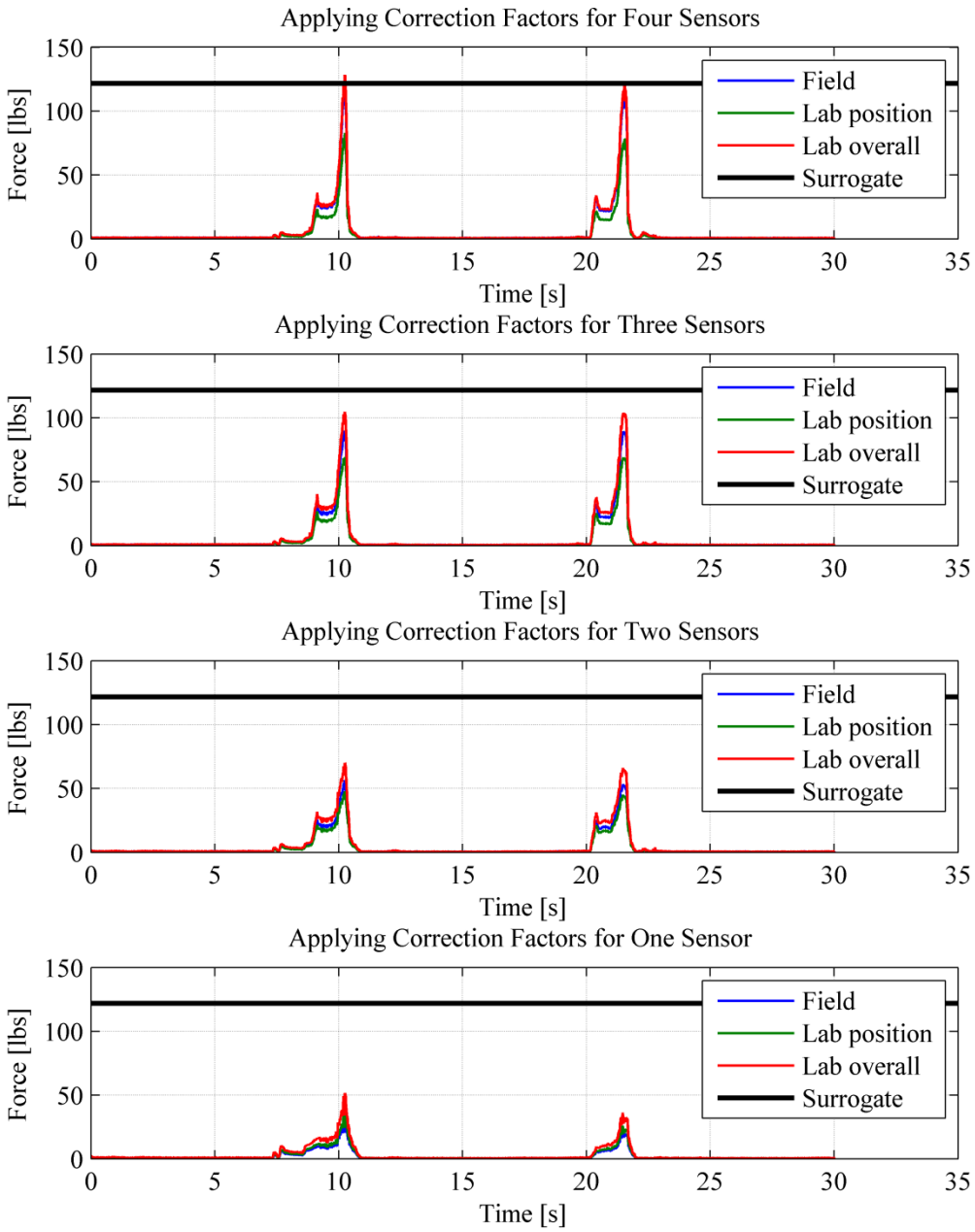

Figure 37: Application of the three models - field subject specific (Field), lab position specific (Lab position), and the overall lab model (Lab overall) conversion factors for Subject A for four, three, two and one sensor (The black line is the average of the peaks of the surrogate measurement (Surrogate). The subject had FlexiForce sensors at locations 1, 2, 7 and 18 according to Figure 20. The tool is a rivet gun and cut resistant gloves were used)

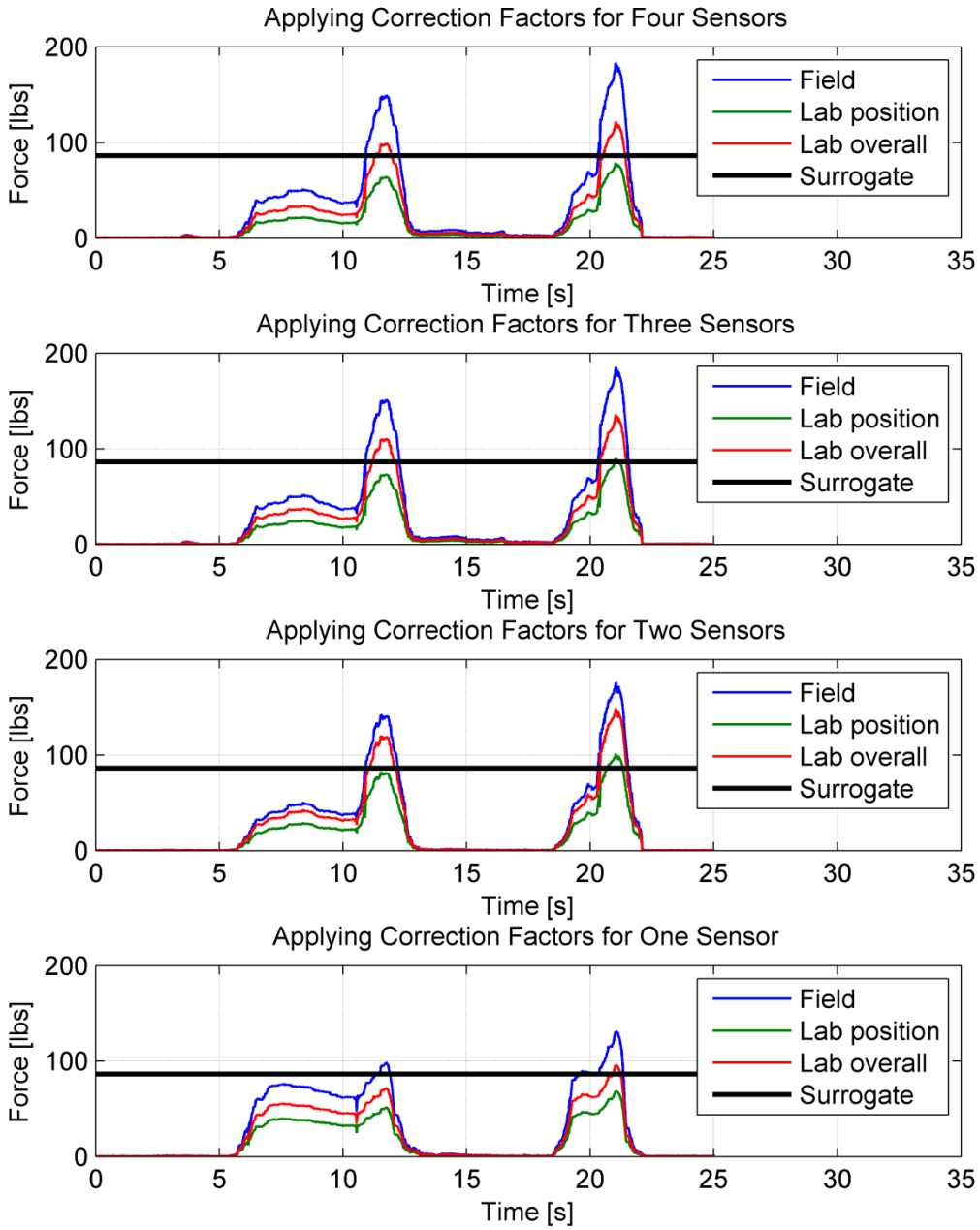

Figure 38: Application of the three models - field subject specific (Field), lab position specific (Lab position), and the overall lab model (Lab overall) conversion factors for Subject B for four, three, two and one sensor (The black line is the average of the peaks of the surrogate measurement (Surrogate). The subject had FlexiForce sensors at locations 1, 6, 7, and 21 according to Figure 20. The tool is a cherry gun and cut resistant gloves were worn)

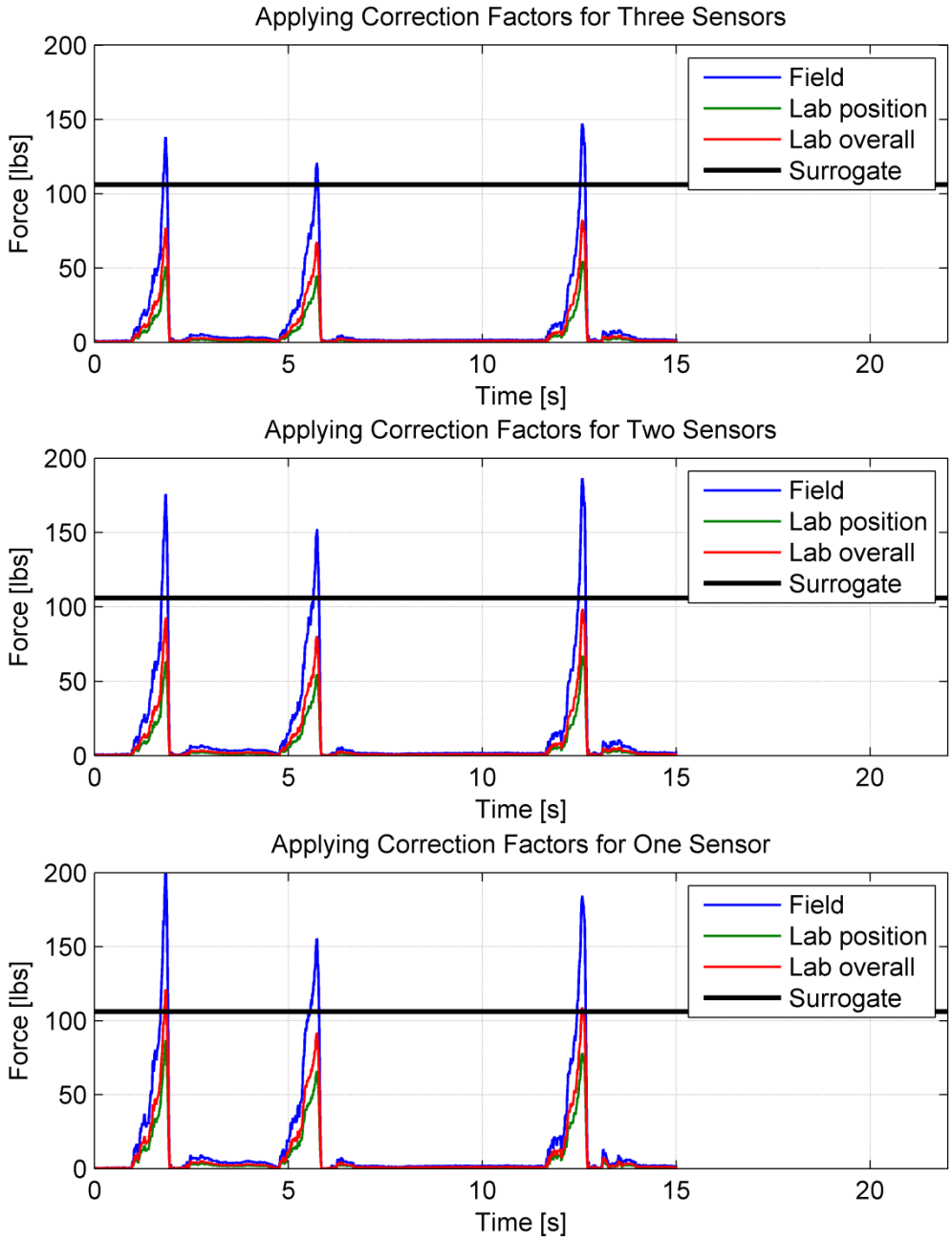

Figure 39: Application of the three models - field subject specific (Field), lab position specific (Lab position), and the overall lab model (Lab overall) conversion factors for Subject C for three, two and one sensor (The black line is the average of the peaks of the surrogate measurement (Surrogate). The subject had FlexiForce sensors at locations 1, 2, and 13 according to Figure 20. The tool is a rivet gun and no gloves were worn)

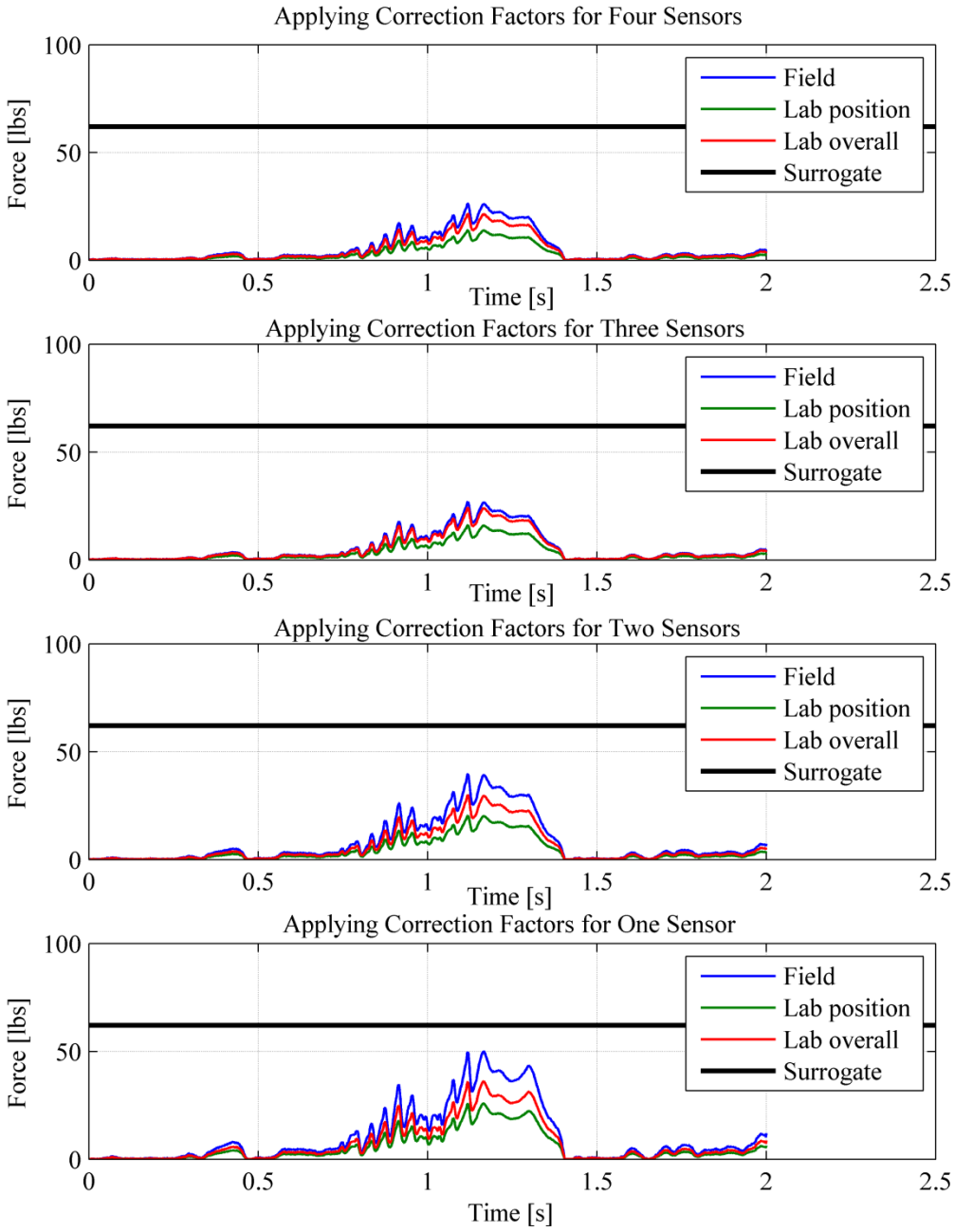

Figure 40: Application of the three models - field subject specific (Field), lab position specific (Lab position), and the overall lab model (Lab overall) conversion factors for Subject D for four, three, two and one sensor (The black line is the average of the peaks of the surrogate measurement (Surrogate). The subject had FlexiForce sensors at locations 1, 2, 14, and 17 according to Figure 20. The tool is a bucking bar and gripping, cut resistant gloves were worn)

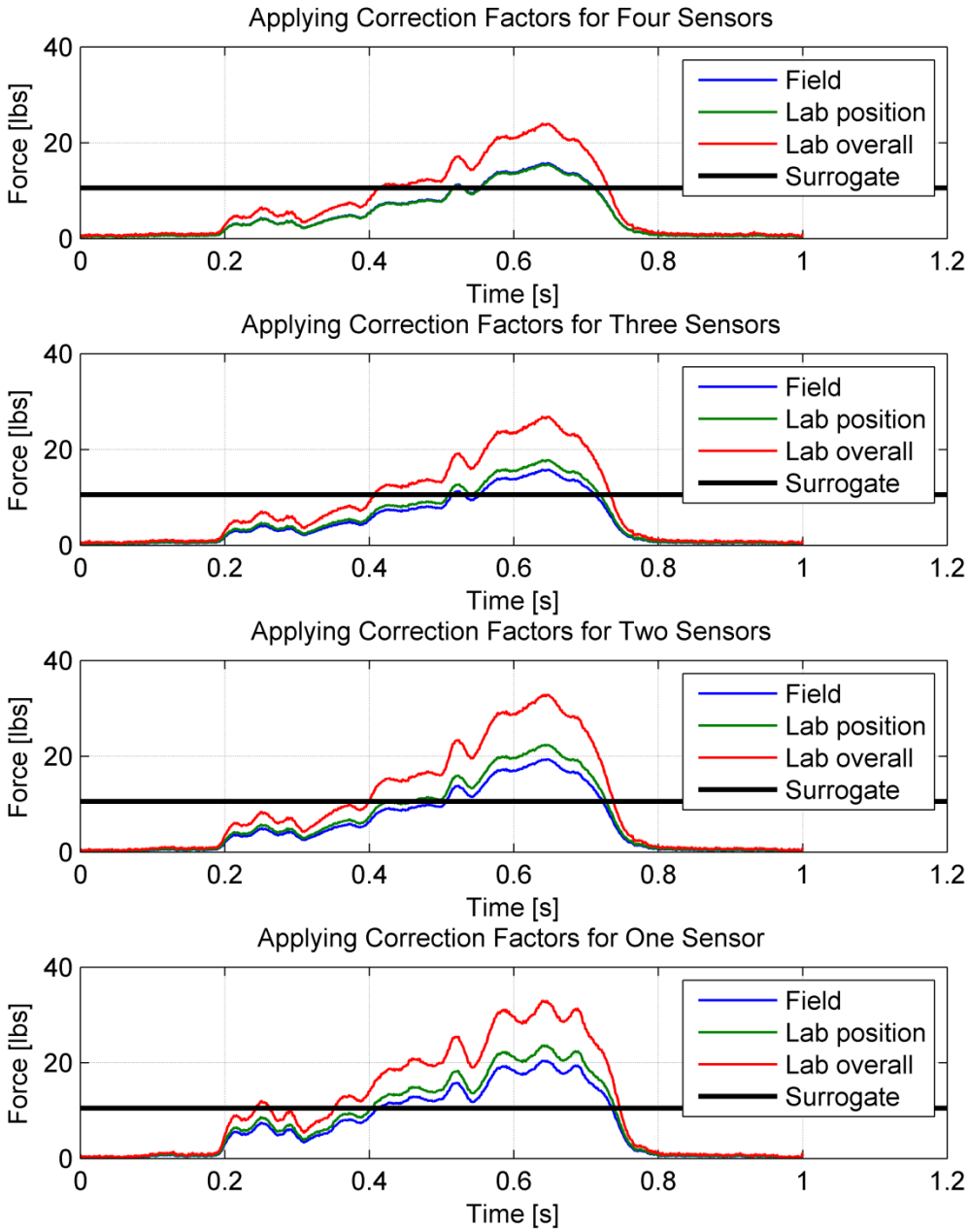

Figure 41: Application of the three models - field subject specific (Field), lab position specific (Lab position), and the overall lab model (Lab overall) conversion factors for Subject E for four, three, two and one sensor (The black line is the average of the peaks of the surrogate measurement (Surrogate). The subject had FlexiForce sensors at locations 2, 3, 5 and 17 according to Figure 20. The tool is a nutrunner and cut resistant gloves were worn)

An alternative method to calculate total grip force estimations was to use the conversion factor of each individual sensor position, which allows for any combination of sensor positions used in the calculation of the grip force. The individual conversion factors are found by using just one FF sensor force reading and dividing it into the force measured from the NIOSH instrumented handle. When combining multiple sensor positions, any sensor position combination can be calculated and each sensor has its own weighting factor. In order to determine which positions are the most common and important, all of the sensor positions used in the field were tallied to form a 'hand histogram', shown in Figure 42. It should be noted that in order for a sensor location to be counted, it needed to have some signal response; therefore, 'silent' sensors were eliminated from the count.

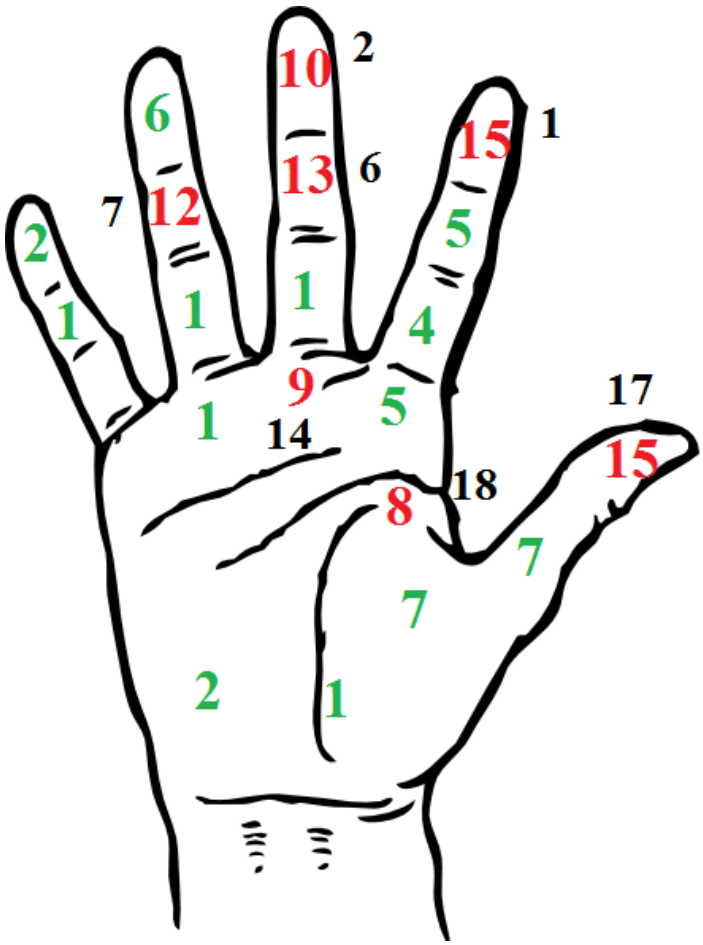

Figure 42: Count of sensor positions used in the field (The red numbers indicate the most common seven positions that were analyzed while green indicate positions that were less common. The black indicators correspond to Table 7)

Using the seven most common positions, pictured in red in Figure 42, the same five subject examples were re-analyzed, since their sensor positions are contained within the seven most common positions of all field measurements and allow for the individual model to be applied. The conversion factors for these seven sensor positions can be seen in Table 8. With subjects A through E being analyzed by both methods, comparisons can be made between them. The results for the five field tool estimations, based on the individual sensor locations conversion factors (Lab Individual), can be seen in Figures 43 through 47. The surrogate measurement (Surrogate) was used as a comparison in each of the subjects presented with the peaks of the surrogate measurements averaged together

and indicated by a black horizontal line. Recall that the surrogate measurement was when the subject grasped the handle immediately after using their tool at the same force that they felt they exerted when using the tool. Although the surrogate is not guaranteed to be accurate, it was used as a reference between the models.

Table 8: Lab conversion factors for the individual sensor positions (Marked red in Figure 42)

	1	2	6	7	14	17	18
Mean	28.30	39.03	76.59	119.51	151.34	94.85	60.07
St.Dev	17.09	25.73	66.29	41.34	74.40	79.88	36.67

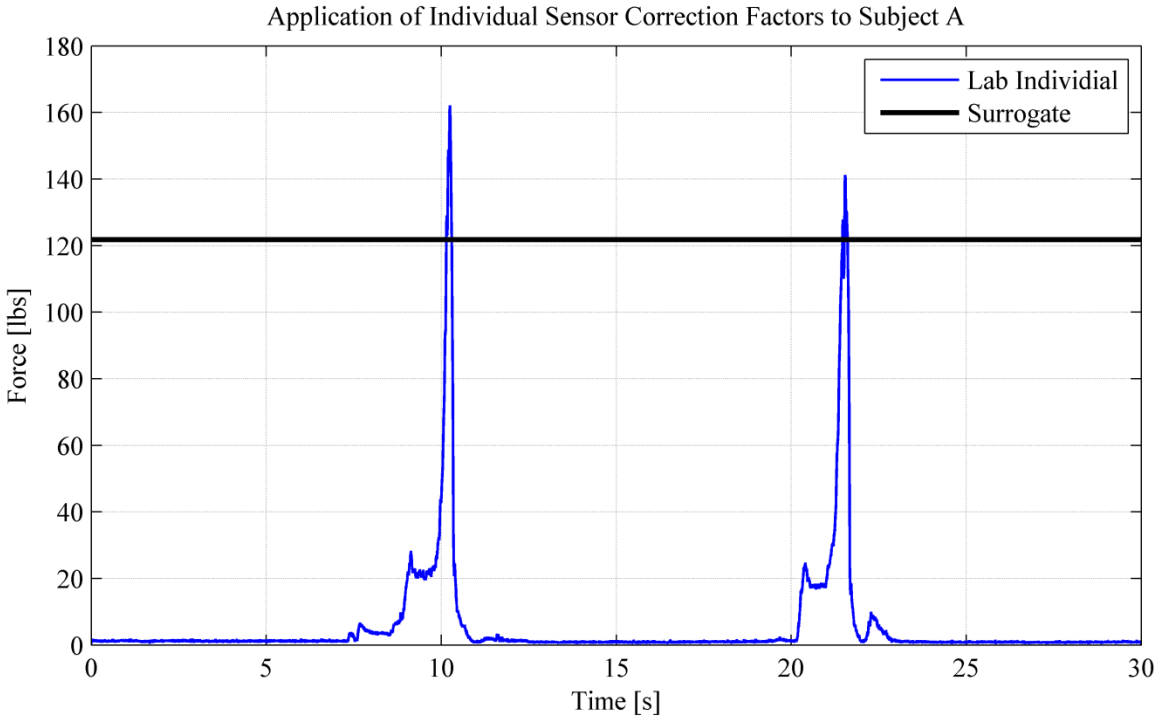

Figure 43: Subject A tool use force estimation based on the individual sensor locations conversion factors (The black line is the average of the surrogate measurement peaks. The subject had FlexiForce sensors at locations 1, 2, 7 and 18 according to Figure 20. The tool is a rivet gun and cut resistant gloves were worn)

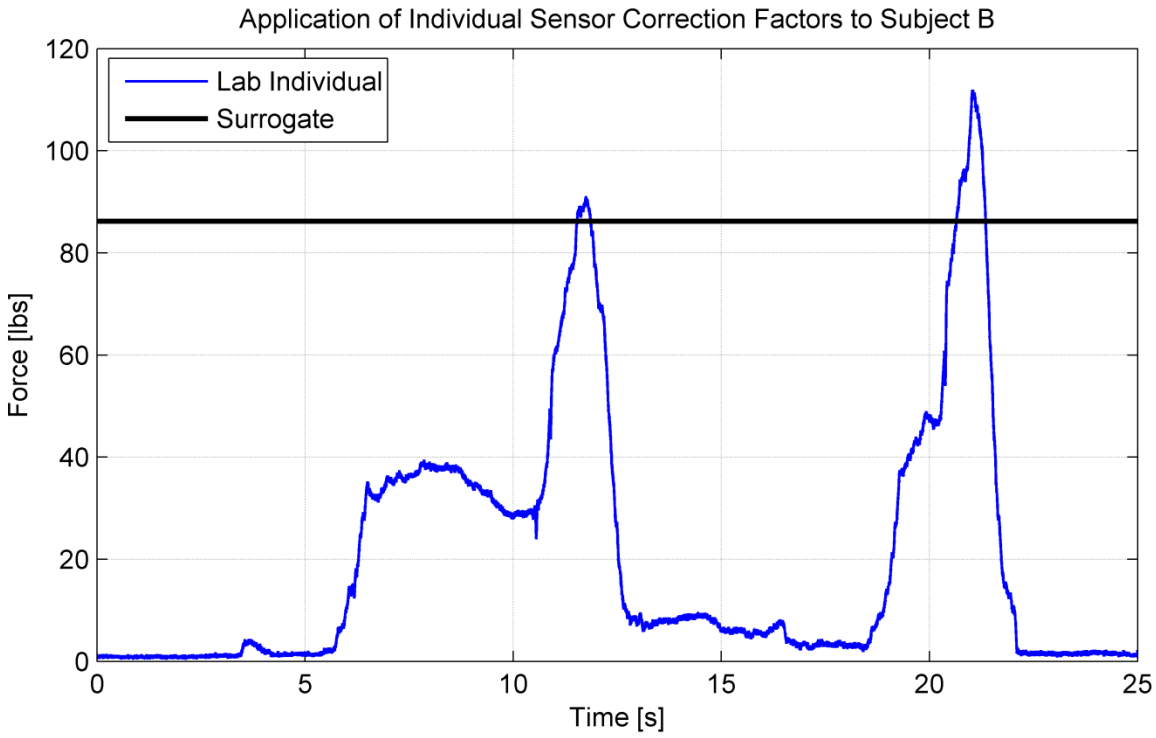

Figure 44: Subject B tool use force estimation based on the individual sensor locations conversion factors (The black line is the average of the surrogate measurement peaks. The subject had FlexiForce sensors at locations 1, 6, 7, and 21 according to Figure 20. The tool is a cherry gun and cut resistant gloves were worn)

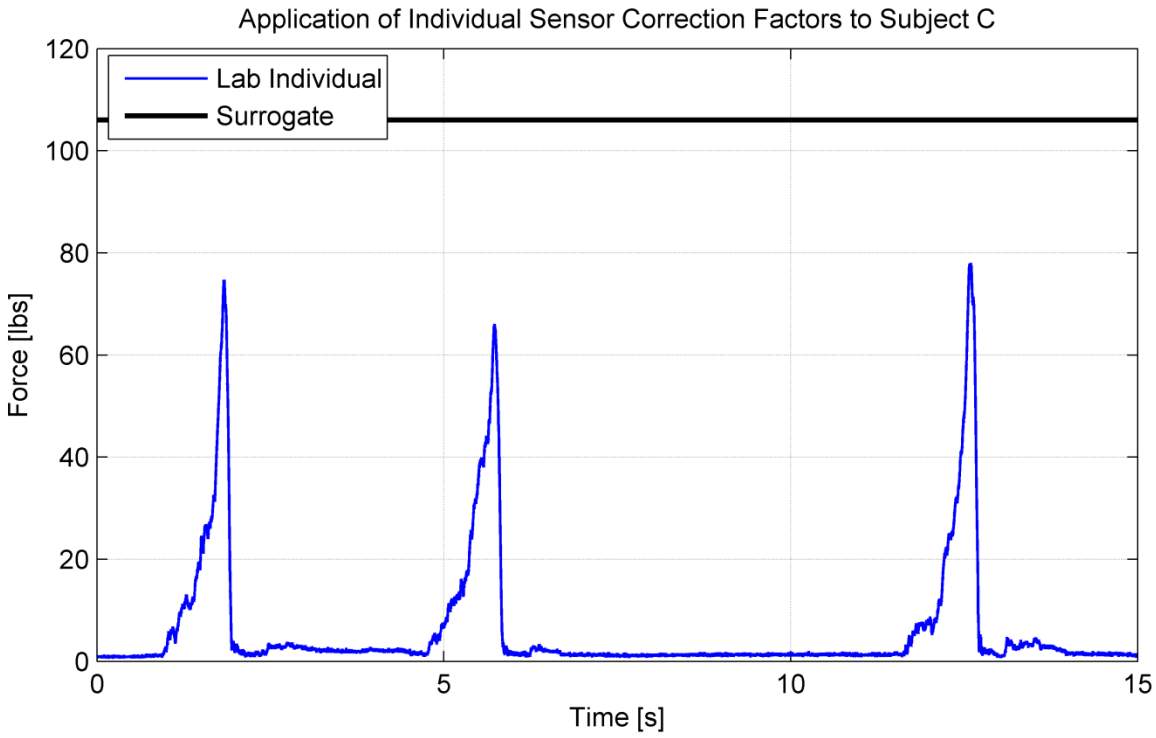

Figure 45: Subject C tool use force estimation based on the individual sensor locations conversion factors (The black line is the average of the surrogate measurement peaks. The subject had FlexiForce sensors at locations 1, 2, and 13 according to Figure 20. The tool is a rivet gun and no gloves were worn)

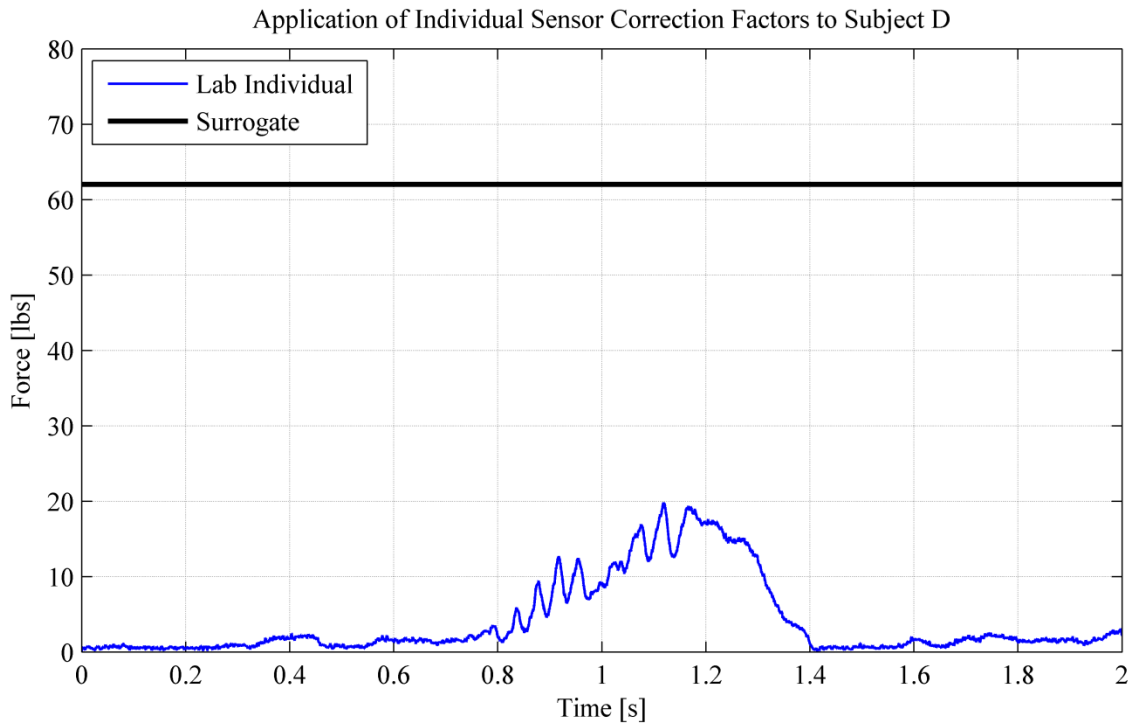

Figure 46: Subject D tool use force estimation based on the individual sensor locations conversion factors (The black line is the average of the surrogate measurement peaks. The subject had FlexiForce sensors at locations 1, 2, 14, and 17 according to Figure 20. The tool is a bucking bar and gripping, cut resistant gloves were worn)

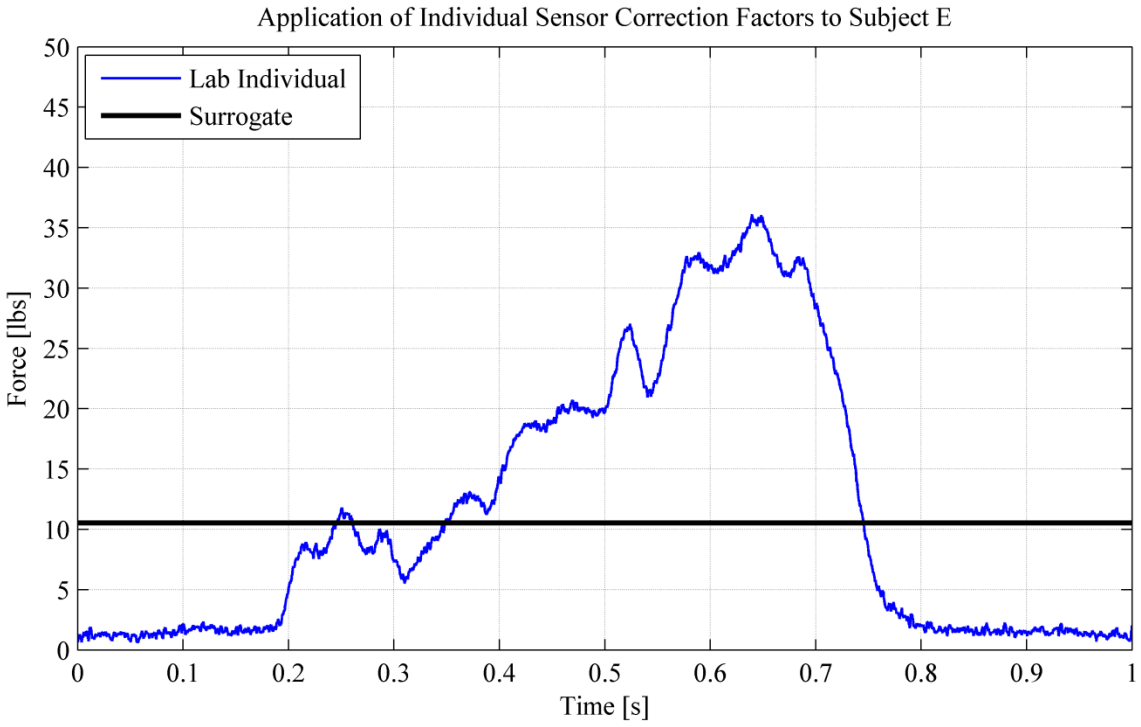

Figure 47: Subject E tool use force estimation based on the individual sensor locations conversion factors (The black line is the average of the surrogate measurement peaks. The subject had FlexiForce sensors at locations 2, 3, 5 and 17 according to Figure 20. The tool is a nutrunner and cut resistant gloves were worn)

The tools that have been collected in the field can be used to develop a template for future field measurements based on the type of grip used for each tool collected. The three tool grip categories analyzed here were the pistol grip, the straight (inline) grip, and the bucking bar grip. It should be noted that the bucking bar category can vary greatly as there are many different types of bucking bars, where each bar needs its own specific grip, which often changes during use. The templates that have been developed for each type of grip can be seen in Figure 48.

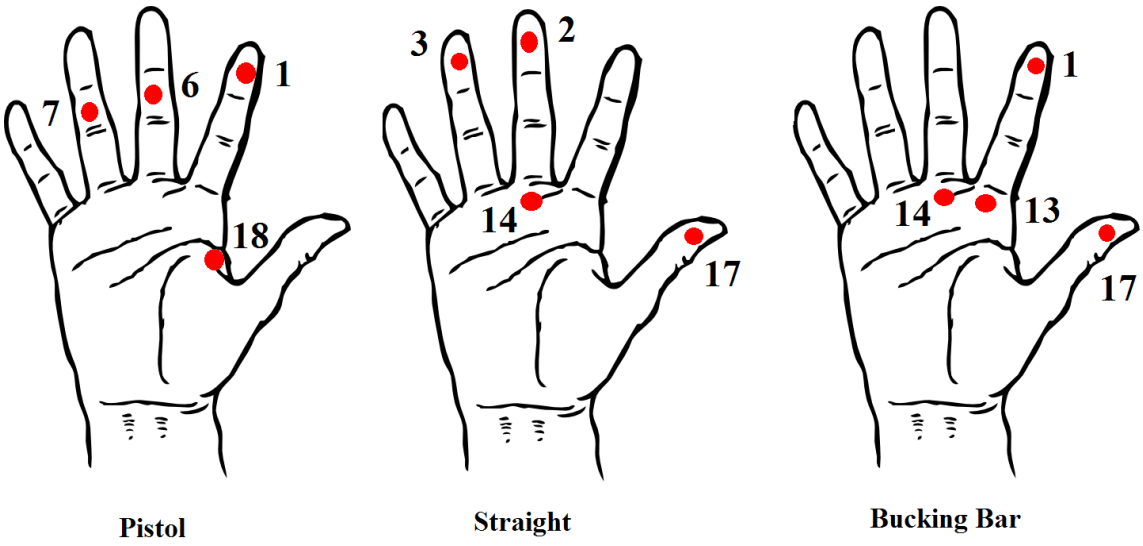

Figure 48: The templates created for the three tool grip categories: pistol grip, straight grip, and bucking bar (Black number correspond to Table 9)

The templates were developed by analyzing the tool grips that have been collected and tallying the most common sensor positions per grip and the most common four sensor positions per grip type. The templates developed can make choosing sensor locations and calculating the estimated grip force for each tool simpler. The conversion factors for the individual sensor positions shown in Figure 48 can be seen in Table 9. In table 9, some of the conversion factors vary greatly between subjects such as in positions 6, 13, and 17, given by the large standard deviations, relative to the mean. This may be due to hand size or handle size.

Table 9: Mean and standard deviation of each of the conversion factors for the sensor positions shown in Figure 48 (Numbering corresponds to Figure 48)

	1	2	3	6	7	13	14	17	18
Mean	28.30	39.03	41.98	76.59	119.51	59.45	151.34	94.85	60.07
St.Dev.	17.09	25.73	22.36	66.29	41.34	43.12	74.40	79.88	36.67

Tables 10 and 11 summarize the different methods and models presented in the study. Table 10 compares the direct field calibration results with the surrogate

measurements made in the field, while Table 11 compares the laboratory models developed with the surrogate measurements. The values within the table are the peak ranges taken from the measurements of each model, where the individual model from the lab was when the conversion factor from each sensor position was used to calculate the total grip force.

Table 10: Summary of the field calibration estimated peak force ranges for the five example subjects compared to the surrogate measurements done with the instrumented handle. (Units in lbs.)

Subject	Type of Grip	FF Field	Surrogate
A	Pistol	80-110	121
B	Pistol	150-180	86
C	Pistol	130-150	106
D	Bucking Bar	25	62
E	Straight	18	10.5

Table 11: Summary of the lab - estimated peak force ranges for the five example subjects compared to the surrogate measurements done with the instrumented handle. (Units in lbs.)

Subject	Type of Grip	Lab Position	Lab Overall	Individual	Surrogate
A	Pistol	60-90	100-120	140-160	121
B	Pistol	60-80	100-110	90-110	86
C	Pistol	50-70	70-90	70-80	106
D	Bucking Bar	20	25	40	62
E	Straight	18	22	20	10.5

For the field calibration, the lab position, and the lab overall models, there are multiple interpretations depending on the number of sensors used. The values used in Table 10 and 11 are conservative, picking ranges used by the three and four sensor combinations.

4. Discussion

4.1 Portable Force Unit

The portable force unit was required to work properly for at least an eight hour day of recording in the field and the battery life test (Figure 22) indicated the batteries took 45 hours to drain the voltage to less than eight volts. At this point, the regulator will still operate, but only until the drop-out voltage of 6.5 V is reached. Anything under this level causes the regulator to stop supplying the 5 V to the op-amps, which stops the unit from working. Forty-five hours is more than five times the minimum requirement for battery life.

Figure 23 shows the frequency response of the low pass filter in stage two of the unit's circuit. The theoretical filter specifications are 1.5 dB lower than the actual tested results in the regions of interest; however, this is explained by component tolerances and is considered acceptable for the purposes of the unit. The noise levels of the unit are small as Vrms is 0.7 mV and Vpp is 8.9 mV, which is roughly seven analog-to-digital conversion steps on a 12-bit ADC. The low noise levels will not interfere with the recordings made on this device. The dynamic range test verified that, with a force of 100 lbs., the voltage output will be 5 V, which, maximize the resolution for the force values in the range of interest. It should be noted that each sensor and each channel are slightly different, due to component tolerances, and may alter the voltage output. All of the specifications that were required of the unit have been met and confident measuring has been verified using the unit for experimentation in both the laboratory and in the field.

4.2 Laboratory Experiments

Using seven subjects as the sample size created issues when testing certain variables such as hand size. For this study, the balance of gender and hand size was as evenly distributed as possible, given only seven subjects (see Table 2),and the ages of the subjects were all very similar as each subject was within six years of the rest of the subjects. The estimated hand areas, using a method adopted from Seo et al. (2008), gave a range for small, medium, and large hand sizes with respect to the fiftieth percentile (Chengalur, 2004), as seen in Table 3 and Table 4, allowing for the categorization of hand size for the subjects used.

Plotting total grip force, given by the instrumented handle, with the force supplied by the FF sensors, shows that there is some scaling factor associated between the two methods of measuring force. This is demonstrated in Figure 24 by plotting the instrumented handle force on the left vertical axis and the varying summations of FF sensor forces on the right vertical. The approach to study and model a conversion factor that can be applied to the FF sensors to estimate the total grip force was generated from a preliminary study yielding similar information as Figure 24. For example, in Figure 24, where the handle recorded 80 lbs., some of the combinations of FF sensors read 20 lbs., giving a conversion factor of four. This example is position and subject specific which makes the overall model more complex than simply correlating the two vertical axes with a scaling factor. The factor that relates the data of the two different measuring techniques was the ultimate parameter of interest.

The individual results from each trial in Figures 25 through 31 give an idea of how the grip from the seven subjects responds to the sensor placement. Figure 30 is the

summary of Subject 6 and it is clear that the DP positions and the MCP joint positions have the lowest conversion factors and the highest contact force. These two positions also have the smallest standard deviation error bars, indicating the most consistency and reliability. If Figure 31 is examined, which is the summary for Subject 7, the same trends appear that were present in Subject 6. The DP and MCP positions have the lowest conversion factors as well as the smallest standard deviations, the thenar and hypothenar position conversion factors are average, and the worst positions, in terms of contact force, are the medial and proximal phalange positions. This trend continues to be the case for majority of the subjects. It is important to note that for all of the subjects, the DP and the MCP joint trials are very similar, which adds validity and repeatability to the tests since these two positions have the same sensors in the same locations for all subjects. Figure 32 is a summary of all of the subjects averaged together and provides a better comparison between positions. The standard deviation error bars indicate the trials that are more consistent and reliable in terms of contact force. From highest to lowest they are: MCP and DP, thenar aspect of the palm, hypothenar aspect of the palm, MP, and PP. Recall that the thenar region contained the distal phalange of the first digit and the hypothenar region contained the proximal phalange of the first digit.

To show how the conversion factors change between subjects numerically rather than graphically, the average conversion factor of all the subjects, based on the number of sensors used, is presented in Table 5. Table 5 shows that the use of eight to four FF sensors yields conversion factors of 11 or 12. This demonstrates that there is not a substantial difference between using eight FF sensors or using four FF sensors, as the estimated force response will be nearly the same for both. Other than using one sensor,

there is little variation amongst the subjects, which indicates repeatability and consistency.

Further analysis was done on the conversion factors in terms of subjects, but grouped by hand size. Each subject's conversion factors were averaged with the rest of the subjects in their hand size category and presented in Table 6. These results indicate that the smallest hand sizes have average conversion factors, the medium hand sizes have the lowest conversion factors, and the large hand sizes have the highest conversion factors. The conversion factors for small and medium hand sizes are closer to each other when compared to the conversion factors of the small and large hand sizes. With a subject pool of seven, it is difficult to draw significant conclusions from this data since the small and large hand sizes only have two subjects each; however, the conversion factors of larger hand sizes were observed to be the highest and suggest a relationship between the contact area of the hand and the distribution of the forces read by the thin-film sensors. Testing with additional subjects is required in order to validate this observation.

Analysis of each trial revealed the force distribution patterns for each subject. The subjects data for each trial were then averaged together to form an overall force distribution pattern per sensor location, presented in Figure 33. Each trial was run separately and the forces vary from trial to trial; therefore, no overall force distribution was calculated. Viewing Figures 33a-c it is clear that the bulk of the force is accounted for on digits two and three, while digit four accounts for some of the grip force and digit five has little to no force readings. When analyzing the palm and first digit, the second digit's MCP accounts for majority of the force across the MCP. The first digits force

readings are stronger at the proximal phalange than at the distal phalange but this may be related to the handle thickness and subject hand size, which when combined, determine where the first digit's distal phalange is positioned during grasping.

These results agree with other published results on grip force distribution. Amis et al. (1987) investigated isometric cylindrical grasping of the hands and found that as the diameter of the handle increased, the normal force decreased and the shear forces shifted towards the distal phalanges. In all cases, the distal segment of the finger imposed force significantly higher than the middle and proximal segments. Amis et al. also found that from digit two to five the contributions of the force recorded, in terms of percent, were as follows: 30%, 30%, 22%, and 18%. In this study, when comparing the forces of just the phalanges, the results from the second digit to the fifth digit were: 37%, 31%, 24%, and 8%. In addition, the second digit accounts for slightly more force and the fifth digit accounts for less force than what Amis reported. To better understand the relationship between this study and other published results, Table 12 is presented.

Table 12: Force distribution among the phalanges of digits two through five from several sources in comparison to the results from this study

Force Distribution by Digit	Second Digit	Third Digit	Fourth Digit	Fifth Digit
This Study	37%	31%	24%	8%
Amis et al. (1987)	30%	30%	22%	18%
Radhakrishnan et al. (1993)	31%	33%	22%	14%
Talsania et al. (1998)	25%	35%	26%	15%

The same patterns are seen in the other published results as seen in this study; however, it should be noted that, in the other studies, the handle size varied (Amis (1987), Radhakrishnan (1993), and Talsania (1998)), while it was held constant in this study. Lee et al. (1991) also found that the total finger force increases as cylinder size

decreases and the phalangeal force centers are not located at the midpoint of the phalanges, but are at the distal phalanges, which agrees with the findings of this study.

To test the capabilities of the models, some of the subjects performed tests where data were not used to develop the models. These tests serve as trials to determine how accurately the model represent total grip. Figure 34 is an example of one of the trails, where the handle is plotted in black and the models are compared to it. By viewing the plot, it appears that the subject specific calibration model was not a good fit. This is explained because the subject specific fit takes into account all of the different positions and this test happens to be a DP position, which has the best contact response; therefore, by averaging in the other positions, the model overshoots.

The same explanation can be applied to the overall average of all subjects. The models that seem to fit best are the subject and position specific model as well as the position specific model. The subject and position specific model is expected to fit the best, since it was designed for this subject in this position; however, this model is impractical for general use because, in order to have the subject and position specific models, a calibration has to be done beforehand with each subject gripping the exact same way as they grip the tool. This is sometimes impossible based on the tool's design and then applying it to the handle. The position and overall model can be applied without the subject calibration and is easier to apply for field measurements.

4.3 Field Measurements

The field measurement protocol differed from the laboratory protocol in terms of the calibration, such that each subject was asked to grip predetermined target grip force values of 20, 40, 60, 80, and 100 lbs. in a randomized order. This gave five reference

points to apply a best fit and allowed for the determination of a field subject calibration conversion factor. If the subject wore gloves while using their tool, they were asked to wear the gloves during the calibration process as well to be as accurate as possible. Using this method, rather than finding a best fit for the entire curve such as in the lab, may result in different conversion factors.

The mounting of sensors in the laboratory also differs from the field, where the sensors were loosely placed between the subject's hand or glove and the handle or tool. This allows for the possibility of sensor slippage and false readings. Subject C's calibration is shown in Figure 35 as an example, where it is evident that the subject had difficulty reaching and maintaining some of the specific target values. This was typical, especially for 100 lbs. force, which is considered a high grip force. Subject C was observed to achieve far greater than 100 lbs. but fluctuated while attempting to maintain it. In theory, this should not matter as the thin-film sensors match the waveform of the entire response. It should be noted that Subject C used three FF sensors and all three are seen matching the behavior of the instrumented handle reference force.

Figure 36 shows a sample of the tool use graph accounting for 30 seconds of the test and shows six tools cycles for Subject C, whose calibration was shown in Figure 35. It is clear from the figure that FF sensor three has the best response followed by FF sensor one and finally FF sensor two. Summing the FF sensors recordings and applying the different models conversion factors, estimations of the total grip force were calculated.

The conversion factors for the lab trial, which had sensor locations most similar to the sensor placement in the field for each of the fives tools presented as an example, was

used as a position model comparison along with the overall model and the field calibration conversion factors (see Table 7). This gives three sets of conversion factors used per subject and tool combination compared with the surrogate measurements.

Applying the conversion factors to samples of each subjects' tool use, results in the plots that are shown in Figures 37 through 41. Subject A is shown in Figure 37 and it appears that the lab overall model best matched the surrogate measurement for the four sensors used, while the lab position model, which was DP, underestimated by a considerable amount and the field subject calibration was less of an underestimation. For all three models, the estimations become less accurate relative to the surrogate as the number of sensors involved in the model decreases. When only one or two sensors were used, the estimations are half of the surrogate measurements; therefore, for Subject A, four sensors most accurately model the estimated grip force when compared to the surrogate measurement.

Figure 38 shows Subject B's tool use, where it was seen that the field subject calibration model overestimated for each number of sensors used. For Subject B, the sensor positions were most similar to that of the MP trial, so the lab MP trials conversion factors were applied. The field calibration model overestimation may be explained by the sensors on the MP responded best with the tool; however, it was shown in the lab that this position leads to poor contact with the handle. Better contact ensures higher force readings for the tool data, which the calibration data lacked, and leads to subject specific conversion factors that overestimate. The lab overall model was also observed to overestimate but not by as much as the field calibration model. The most accurate model was the lab position model, which was the MP position. When the models are applied

with just one sensor, the lab overall model fits best. All these observations are made with the assumption that the surrogate measurement was the most accurate measurement of tool grip force.

Subject C's tool grip force estimation data is presented in Figure 39. This is the same subject whose calibration and tool recording are shown in Figures 35 and 36 as examples. The subject specific field calibration model gives the highest estimated force and supports an idea that, during the calibration, the gloves may have influenced the FF sensors readings. It should be noted that Subject C used three FF sensors unlike the other subjects who used four. As the number of sensors used in the models decreased, the model estimations increased. This was interpreted as one FF sensor responsible for majority of the force response during tool use versus in the calibration all three sensors were contributed to the total force. The lab overall model seems to fit best with the use of one sensor in the model.

Subject D's tool grip force estimation data is presented in Figure 40 and was the first subject to use a non-pistol grip tool. Subject D used a bucking bar and the MCP lab position trial was used due to sensor placement agreement with the bucking bar grip. The same pattern of the field calibration subject specific model having the highest estimations was present again followed by the lab overall model and then the lab positional model; however, all of the models underestimate grip force based on the surrogate measurement. The sensor placement and recording during a bucking bar tool measurement was difficult, since the subject was constantly adjusting the tool and changing grips leading to FF sensor slippage and false readings. It is interesting that, as the number of sensors used

decreases, the models become more accurate. This may be explained by one sensor registering the bulk of the force readings.

Subject E is presented in Figure 41 and used a straight (in-line) tool. In the figure, the low surrogate force measurement is obvious. A grip force of 10 lbs. was very small and may not be accurate due to bias. Subject E was the first example where the overall lab model had the highest estimated grip force and the field subject calibration model has the lowest, which was off by 10 lbs. from the surrogate. The conversion factors of the DP lab trial were used for Subject E due to sensor placement agreement.

It is important to remember, for all subject data presented, there was a protocol difference from the field to the lab. When in the field, the majority of the subjects wore gloves, where some gloves were padded and others were thinner and used for cut-resistance. The padded gloves were used to absorb some of the vibration from the tools, while the cut-resistant gloves were for protection and safety and a third type of glove with rubber tips was used for better gripping. Depending on the type of glove used, the thickness of the glove and material of the glove, the FF sensor readings were likely influenced. This may explain some of the differences in estimations between the models and the surrogate measurements. Recall that in the field the sensors were placed between the glove or hand and the tool or handle, which may allow for slippage and false readings.

When analyzing the field subject results with the alternative method, based on the laboratory individual sensor position conversion factors the results are comparable to the best contact response method. The most common sensor locations used in the field are seen in Figure 42 and the corresponding conversion factors for each location are

displayed in Table 8. Using the most common seven FF sensor positions, Subjects A through E were re-analyzed to estimate the tool grip force. For Subject A (Figure 43), the alternative method gives a tool grip force similar to the surrogate measurement; however, the alternative method of individual sensor is slightly higher than the surrogate measurement.

Subject B's tool use grip force estimation based on the alternative method (Figure 44) shows that the model was close to the surrogate measurement; however, the estimation was slightly higher than the surrogate, again. In Figure 45 for Subject C the surrogate measurement is higher than the estimated force but, since the surrogate measurement registers over 100 lbs. force, which is a substantial grip force, there may be bias in the measurement.

Figure 46 displays Subject D's bucking bar estimated grip force based on the individual sensor model. The model estimations were significantly lower than the surrogate; however, it is important to note that, in the averaging of the peaks for the surrogate measurement, there were fluctuations from 50 to 80 lbs., which may indicate uncertainty or bias. Figure 47 contains Subject E's individual model estimation, which was overestimated. As mentioned previously in this section, the surrogate measurement was only 10 lbs., which was a weak grip force and likely to be an underestimation.

By analyzing the collection of tools and their respective FF sensor locations, templates were designed for three types of grips used, shown in Figure 48 and the respective conversion factors in Table 9. Using these templates, and their individual sensor conversion factors, should make future field investigations simpler.

In the results section, Tables 10 and 11 summarize the results of the different methods and models presented in this thesis. The values in the tables are estimated peak force ranges from the measurements and models. Table 10 contains the field subject model compared to the surrogate measurements. In three of the five example subjects, the subject calibration model is higher than that of the surrogate measurement. Table 11 contains the lab position model, the lab overall model, and the individual sensor model compared to the surrogate measurements. In four of the five tools, the lab position measurement is lower than the field surrogate measurement. The lab overall and lab individual models are in closer agreement with the surrogate measurements. For both models, there are two over estimations, two underestimations, and one accurate estimation. These observations are based on the surrogate measurement being the true reference grip force; however, it is naive to think that the surrogate measurement is 100% correct and there was no bias on the subject's behalf.

Overall, the different calibrations and methods model the subjects and their tools adequately. There are many factors that influence each model to become more or less accurate with respect to the surrogate measurement and to each other. Some of these factors are readily explained, such as the types of gloves worn: rubber gloves for grip, cotton gloves for safety and protection, and padded gloves for anti-vibration. The thickness and materials used in the gloves may influence the readings of the FF sensors. A second possible influence was the change of protocols from the laboratory to the field. The field calibrations had predetermined target grips with a five point calibration; whereas, the laboratory subjects were asked to grip up to 80% of their maximum grip force at a steady rate to allow for a best fit of the entire waveform. The two methods of

curve fitting the calibrations may yield different results. Another possible protocol issue is the method of mounting sensors, where, if the sensors are secured with tape, they may yield better results. Finally, in the laboratory the tests were performed entirely on the NIOSH instrumented cylindrical grip force handle, while in the field, even though the calibration was done on the handle, the actual measurement was done on the tool and many tools were studied with different grips. Each time a tool that varied from the shape and size of the NIOSH instrumented handle was used, variability was added. Given these issues, the models still gave consistent and realistic force estimations for the different subjects and tools presented.

5. Future Directions

This study can be used as a stepping stone for future hand grip force experiments. A few improvements that can be made immediately in the laboratory experiments are the addition of more subjects varying in age, gender, and hand size, which will provide more detailed information about the models. A larger subject pool also allows for further investigation into the influence of hand size. One hardware change that can take place is to have one ADC that samples at high rates and has the ability to accommodate all measuring devices used. A second hardware change is to implement handles of different diameters. Many of the studies reviewed used a variety of handle diameters that revealed changes in grip based on handle diameter (Mentzel (2011), Amis (1987), and Radhakrishnan (1993)). Having multiple handle diameters allows for more models based on the tool diameter and increases the accuracy of the models. An expansion on this idea is to use of handles that are non-cylindrical, since not all tools have cylindrical handles and require different grip types. The more the calibration of the models has in common with the actual test, the more accurate they become.

In terms of the unit itself, there are several features that could be improved. For example, circuitry can be redesigned onto a PCB board to significantly reduce the size of the unit, making it even more portable. The components that control the filter specifications in the second stage of the circuitry, can also be put into sockets for additional control and versatility, similar to the gain resistor in the first stage. If the unit developed was expanded to more channels, then the entire hand could be mapped at once, rather than in six separate trials. This allows for direct comparisons between sensor locations that were not included in the same trials and reveal more detailed information

about force distribution. However, the sensor setup would have to be modified, since 32 FF sensors on one hand is impracticable and would influence the grip and grip force data. If this is not an option, an expansion on this study would be to take the eight optimal sensor locations for each subject and run a seventh trial that would give the best conversion factors for optimal contact force. This idea could be expanded and applied to different tool grips in the way this study has done with the grip templates. Another idea regarding grip force distribution is to analyze the individual NIOSH instrumented handle arms for their force readings in each trial to see if there is a correlation with FF sensors placed on each arm. As mentioned by Wimer (2009), the handle has the potential to be used for distribution analyses. The relationship between FF sensors and the instrumented handle in terms of distribution may reveal interesting patterns.

Other changes that could be implemented are simple, such as making the protocols the same so that the calibration process for field measurements and laboratory measurements are identical. Another simple change that can be made, but at the sacrifice of time, is taping the sensors to the subject's hands or gloves. This ensures sensor placement is constant throughout the testing process and eliminates silent sensors or false readings. If some of these improvements are made and the model accurately represents total grip force using thin-film sensors, then the model can be applied to help better understand hand-arm vibration. Whether or not grip force influences the exposure levels of vibration is still unknown, but with improvements, this model has the potential to be accurate enough to discover an answer.

6. Conclusion

The portable force unit that was developed met all of the specified requirements and provides data capturing using eight FF sensors in environments that were previously unavailable due to portability. The unit is used to supply power to the FF sensors, while amplifying and filtering the signals before passing them on to an ADC. This made using thin-film sensors a viable option in the laboratory and in the field for many different applications.

The laboratory study concluded that the distal phalange and metacarpophalangeal joints of digits two through five are the best sensor locations for registering contact force. These results agree with many of the published works in the area of grip force, reinforcing its validity (Amis (1987), Radhakrishnan (1993), Talsania (1998), and Lee (1991)). This study also concluded that a minimum of four thin-film sensors applied to the hand and coming into contact with the object grasped to capture the force distribution is necessary to accurately represent the total grip force; however, it was shown that, although possible with two or three sensors, four sensors yields acceptable accuracy when minimizing the number of sensors used and minimizing sensor bulk.

There are a number of factors that need to be taken into account in order to maximize the accuracy of the models. One of these factors is sensor location, where the minimum of four sensors should be placed in the optimal locations to capture contact force. A closely related factor is the grip type, which is tied to the tool being used. As was seen from field experiments in this study, using one grip for the calibration that is different from the actual test run leads to overestimation or underestimation. It is best to have the same grip used for both measurements to limit the number of variables. Also

seen in the field setting, was the use of gloves. Some gloves have cushion and may absorb some of the force and interfere with thin-film sensor recording, which may lead to overestimations or underestimations. The calibration should be done in the same way that the test is done, therefore if the subject wears gloves during the activity, they should wear gloves during calibration.

Hand size is a factor that still is unclear. Some results from this study indicate that the larger the hand size is, the higher the conversion factor may be. The reasoning behind this is that the thin-film sensors have a fixed sensing area and different hand sizes correspond to different contact areas. The larger the hand size, the larger the contact area, and the less of the total grip force is captured by the constant sensing area of the sensors. Capturing less of the total force by the sensors leads to higher conversion factors that may cause inconsistent estimations between subjects with different hand sizes. One last issue was the difference of protocol between the field and the laboratory experiments. The calibration methods varied such that the best fit for target points in the field may differ from the best fit for an entire waveform, as seen in the laboratory. This is something easily avoided when starting a new experiment as well as the method of securing sensors to the subject's hand or glove.

In conclusion, the models developed and proposed in this study were able to estimate total hand grip force during tool use based on calibrations. Some of the issues mentioned such as protocol changes, gloves, and grip types made some of the data inconsistent, but the ability to produce estimations in an acceptable range is certainly possible. By eliminating the issues, the models become even more accurate, allowing them to be applied and better understand hand-arm vibration. Whether or not grip force

influences the exposure levels of vibration is still unknown, but with improvements, this study's models have the potential, and accuracy, to discover the answer.

REFERENCES

1. Peterson, A. Brammer, and M. Cherniack. "Exposure Monitoring System for Day-long Vibration and Palm Force Measurements." *International Journal of Industrial Ergonomics* 38 (2008): 676–686.

2. Lemerle, P. et al. "Application of Pressure Mapping Techniques to Measure Push and Gripping Forces with Precision." *Ergonomics* 51.2 (2008): 168–191.

3. Mentzel, M et al. "Assessment of Force Patterns of Different Primary Grips Through Dynamic Force Measurement Using a Sensor Glove." Handchir Mikrochir Plast Chir. 43.3 (2011): 155-161

4. Chadwick, E.K.J., and A.C. Nicol. "A Novel Force Transducer for the Measurement of Grip Force." *Journal of Biomechanics* 34.1 (2001): 125–128.

5. Wimer, Bryan et al. "Development of a New Dynamometer for Measuring Grip Strength Applied on a Cylindrical Handle." *Medical Engineering & Physics* 31.6 (2009): 695–704.

6. Ferguson-Pell, Martin, Satsue Hagisawa, and Duncan Bain. "Evaluation of a Sensor for Low Interface Pressure Applications." *Medical Engineering & Physics* 22.9 (2000): 657–663.

7. Lebosse, C. et al. "Nonlinear Modeling of Low Cost Force Sensors." *IEEE International Conference on Robotics and Automation, 2008. ICRA 2008*. IEEE, 2008. 3437–3442.

8. Al Khaburi, J. et al. "Measurement of Interface Pressure Applied by Medical Compression Bandages." *2011 International Conference on Mechatronics and Automation (ICMA)*. IEEE, 2011. 289–294.

9. Ouckama, Ryan, and David J. Pearsall. "Evaluation of a Flexible Force Sensor for Measurement of Helmet Foam Impact Performance." *Journal of Biomechanics* 44.5 (2011): 904–909.

10. Lu, Ming-Lun et al. "An Investigation of Hand Forces and Postures for Using Selected Mechanical Pipettes." *International Journal of Industrial Ergonomics* 38.1 (2008): 18–29.

11. Nikonovas, A. et al. "The Application of Force-sensing Resistor Sensors for Measuring Forces Developed by the Human Hand." *Proceedings of the Institution of Mechanical Engineers, Part H: Journal of Engineering in Medicine* 218.2 (2004): 121–126

12. Marcotte, Pierre, Adieus, Surajudeen, and Rakheja, Subhash. "Development of a Low-Cost System to Evaluate Coupling Forces on Real Power Tool Handles." Canadian Acoustics 39.2 (2011): 36-37

13. Slane, Josh et al. "The Influence of Glove and Hand Position on Pressure over the Ulnar Nerve During Cycling." *Clinical Biomechanics* 26.6 (2011): 642–648.

14. Seo, Na Jin, Thomas J. Armstrong, and Justin G. Young. "Effects of Handle Orientation, Gloves, Handle Friction and Elbow Posture on Maximum Horizontal Pull and Push Forces." *Ergonomics* 53.1 (2010): 92–101.

15. Wimer, Bryan et al. "Effects of Gloves on the Total Grip Strength Applied to Cylindrical Handles." *International Journal of Industrial Ergonomics* 40.5 (2010): 574–583.

16. Ruiz-Ruiz, Jonathan et al. "Hand Size Influences Optimal Grip Span in Women but Not in Men." *The Journal of Hand Surgery* 27.5 (2002): 897–901.

17. Seo, Na Jin, and Thomas J Armstrong. "Investigation of Grip Force, Normal Force, Contact Area, Hand Size, and Handle Size for Cylindrical Handles." *Human Factors* 50.5 (2008): 734–744.

18. Burström, L. "The Influence of Biodynamic Factors on the Mechanical Impedance of the Hand and Arm." *International Archives of Occupational and Environmental Health* 69.6 (1997): 437–446.

19. Lin, Jia-Hua et al. "Forces Associated with Pneumatic Power Screwdriver Operation: Statics and Dynamics." *Ergonomics* 46.12 (2003): 1161–1177.

20. Buchholz, Bryan et al. "Subjective Ratings of Upper Extremity Exposures: Inter-method Agreement with Direct Measurement of Exposures." *Ergonomics* 51.7 (2008): 1064–1077

21. Li, Kai Way, and Ruifeng Yu. "Assessment of Grip Force and Subjective Hand Force Exertion Under Handedness and Postural Conditions." *Applied Ergonomics* 42.6 (2011): 929–933.

22. Dale, A.M. et al. "Variability and Misclassification of Worker Estimated Hand Force." *Applied Ergonomics* 42.6 (2011): 846–851.

23. Eksioglu, Mahmut, and Kemal Kızılaslan. "Steering-wheel Grip Force Characteristics of Drivers as a Function of Gender, Speed, and Road Condition." *International Journal of Industrial Ergonomics* 38.3–4 (2008): 354–361.

24. Lin, Jia-Hua, Raymond W. McGorry, and Jacob J. Banks. "Exposures and Physiological Responses in Power Tool Operations: Fastening Vs. Unfastening

Threaded Hardware." *Journal of Occupational and Environmental Hygiene* 7.5 (2010): 290–297.

25. Gray, Henry, Richard L. Drake, Wayne Vogl, Adam W. M. Mitchell, Richard Tibbitts, and Paul Richardson. *Gray's Anatomy for Students*. Philadelphia: Elsevier/Churchill Livingstone, 2010

26. "FlexiForce® Sensors." *FlexiForce Force Sensors*. Tekscan. Web. 20 Apr. 2012. <http://www.tekscan.com/flexible-force-sensors>.

27. Mancini, Ron, and Bruce Carter. *Op Amps for Everyone*. Amsterdam: Newnes/Elsevier, 2009

28. Chengalur, S. N. *Kodak's Ergonomic Design for People at Work*. 2nd ed. Hoboken, NJ: Wiley, 2004

29. Amis, A. A. "Variation of finger forces in maximal isometric grasp tests on a range of cylinder diameters." *Journal of Biomedical Engineering, 9*, (1987). 313-320

30. Radhakrishnan, S., and M. Nagaravindra. "Analysis of Hand Forces in Health and Disease During Maximum Isometric Grasping of Cylinders." *Medical & Biological Engineering & Computing* 31.4 (1993): 372–376.

31. Talsania, J., and S. Kozin. "Normal Digital Contribution to Grip Strength Assessed by a Computerized Digital Dynamometer." *The Journal of Hand Surgery: Journal of the British Society for Surgery of the Hand* 23.2 (1998): 162-66

32. Lee, J.W., and K. Rim. "Measurement of Finger Joint Angles and Maximum Finger Forces During Cylinder Grip Activity." *Journal of Biomedical Engineering* 13.2 (1991): 152–162